Discrete Geometry to Image Processing

Stéphane Marchand-Maillet

Institut EURECOM - B.P. 193 - F-06904 Sophia Antipolis

Contents

Abstract

Image processing operations typically involve processing of data in discrete form. Information given by such data is mostly recovered via the study of inter-relationships between discrete points (*i.e.*, pixels). There is therefore a need for developing a context in which concepts used are kept consistent with this kind of data.

In this paper, we summarise and extend results known in discrete geometry from the construction of a discrete topological concept to the characterisation of geometrical properties of discrete sets of points. The context of binary image processing is taken as a support for illustrating this study. Emphasis is placed on characterising straightness and convexity is discrete spaces. This is done via the definition of discrete distances which are shown to be close to well-known concepts in graph theory. An extended neighbourhood space is also constructed and shown to provide us with more flexibility and compactness than classically used neighbourhood spaces while preserving the possibility of characterising analytically the main geometrical properties of discrete points.

The study developed in this paper can form the basis for different extensions, both regarding the richness of the neighbourhood used and the quantity of information available at each pixel location.

1   Introduction

The use of computers for the development of new technologies has imposed processing of data in discrete form. Information is no longer continuous but rather given at some discrete locations in time or space. This is particular true in the context of image processing where pictures are digitised into pixels. The

global information contained in the image is recovered via the study of inter-relationships between pixels. For analysis of such data, it is therefore crucial to obtain formal discrete characterisations similar to that known in continuous spaces. Discrete geometry is one such field which aims for characterising concepts such as straightness in the discrete space.

In this paper, we first present the construction of a formal context in which such characterisations will be further developed. Advantages of such an approach are illustrated using the context of binary image processing. Then, we recall major results in discrete geometry in relation to the well-studied 8-neighbourhood discrete space. Discrete convexity and discrete straightness are mostly considered here. In a second part, we extend these properties to a newly constructed discrete space. While doing that, we derive some results as to the advantages of such a mapping.

More precisely, the paper is organised as follows. Section 2 presents the particular class of binary images which will be used as a support to our developments. By this mean, this section briefly recalls the underlying structure of most of discrete spaces encountered in image processing.

The identification of image components relies on a connectivity relationship between pixels. This topological context which introduces the concept of neighbourhood between pixels has been developed in the early stages of binary image analysis and is presented in Section 3. In turn, digital topology allows for the definition of connected subsets of pixels such as arcs and curves. We consider connectivity in relation to square lattices. In other words, pixels in the image are arranged on the unit square grid. Such an underlying structure facilitates analytical developments and image storage and remains the most widely used framework. The originality of this study lies in the fact that we will map the digital topology onto a combinatorial structure, the grid graph. This approach has been suggested in [28] and developed in [37]. Image-to-graph mapping provides us with efficient procedures for solving discrete optimisation problems [12]. Moreover, efficient data structures have been created to manage data in this context (*e.g.*, see [6]).

Pixels are now grouped in discrete objects (*e.g.*, paths or connected components) and it is the properties of these subsets that are under study. Two aspects are generally considered for analysis. In order to perform shape characterisations, geometric notions such as straightness and convexity are to be defined in discrete spaces. On the other hand, measurements within the image are necessary. Both discrete geometry and shape measurements therefore rely on the definition of a distance. For consistency with the context in which image analysis operations are studied, purely discrete distances have been proposed. Different approaches are generally taken for their definitions. However, a common framework defines discrete distances using known local distances within a neighbourhood or within combinations of neighbourhoods. Section 4 summarises these advances in relation to the 8-neighbourhood space.

Building on this, Section 5 presents the construction of the 16-neighbourhood space within which equivalent characterisations will be derived. In particular, we introduce two new discrete distances in this space which will form the basis for the development of discrete properties in this space. It is also shown that the approach taken allows for an easy mapping of most of the properties known in the 8-neighbourhood space into the 16-neighbourhood space.

Finally, Section 6 suggests a direct application of these results to the domain of binary image processing.

2 Binary digital images

The acquisition of an image is generally done using a set of physical captors. The acquisition process can therefore be accurately modelled as a sampling of the continuous image using a discrete partitioning of the continuous plane. For the sake of simplicity, only partitions involving regular polygons are considered. That is, polygons with sides of constant length and a constant angle between them. It is easy to show that, for constructing a partition of the plane, only three regular polygon types can be used. The possible numbers of sides of the regular polygon used are three, four and six, leading to triangular, square and hexagonal partitioning schemes respectively (see Figure 1).

In the mathematical model of an image, the pixel area is identified with its centre leading to the representation of pixels as discrete points in the plane. As shown in Figure 2, a lattice can be built which connects all such pixel centres.

The sampling partition is represented with dotted lines and the pixel centres as black dots (●). The lattice represented with continuous lines is dual to the partition in the sense that two pixels are joined in
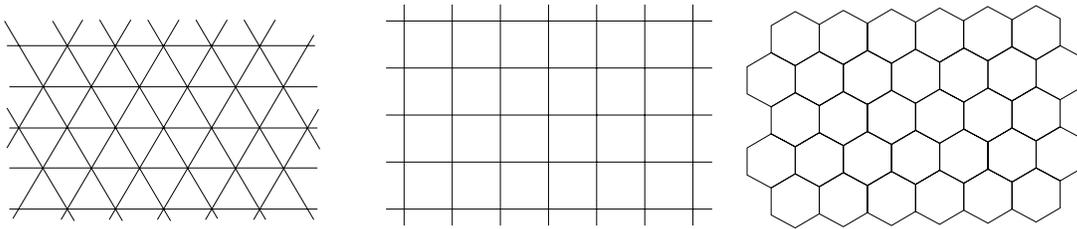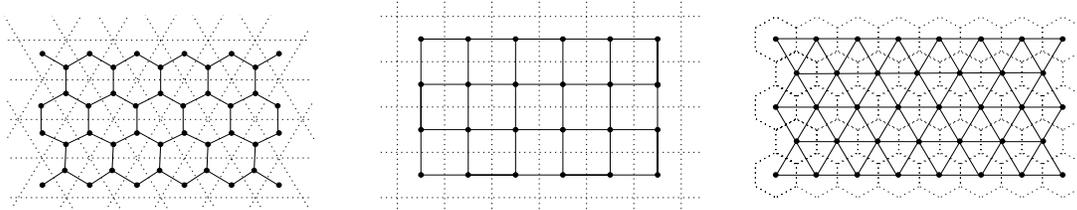
Figure 1: Different sampling schemes

Figure 2: Resulting pixels from sampling shown in Figure 1.

the lattice if and only if the two partition polygons share a common edge. A triangular partition results in an hexagonal lattice. Conversely, an hexagonal partition will result in a triangular arrangement of pixels, the triangular lattice. Finally, for a square sampling of the image, the pixels can be considered as integer points of a square lattice.

Physically, such polygons represent captors sensitive to the intensity of light. Their output is a value on a scale. In a grey scale image, each pixel is therefore associated with a single colour value. Equivalent to the sampling of the spatial domain of the image, the colour scale is sampled using a given number of discrete ranges. We consider grey scale images where the colour scale is one-dimensional. When using only two such ranges representing white and black colours (0 and 1 respectively), we obtain binary images.

As result of the complete acquisition process, a two-dimensional binary image is given as a two-dimensional array of pixels where each pixel is associated with a colour value which can be either 0 (white pixel) or 1 (black pixel). In order to define mathematical tools for picture processing such as connectivity and distance measurement, we need to set a theoretical basis on the discrete set of pixels thus obtained. Digital image processing relies heavily on the definition of a topology which forms the context in which local processing operators will be defined.

In this work, we will specialise in square lattices and partitions since they represent the most suitable case for analytical study. Moreover, it will become apparent that a mapping can be defined that create a relation with other types of regular partition (e.g., triangular partitions).

3 Digital topology

It is commonly known that the discrete topology defined by pure mathematics cannot be used for digital image processing since in its definition every discrete point (i.e., a pixel in the image processing context) is seen as an open set. Using this definition, a discrete operator would consider the image as a set of disjoint pixels only, whereas it is generally admitted that the information contained in the image is stored in the underlying pixel structure and the neighbourhood relations between pixels. Alternative definitions have been proposed. In contrast with classic *discrete topology*, digital image processing is based on *digital topology* [4, 20, 34]. The definition for digital topology is based on a neighbourhood for every point.

Neighbourhoods in digital topology are typically defined by referring to the partition dual to the lattice considered. For a given point, defining its neighbouring points is equivalent to defining a relationship between the corresponding pixel areas in the partition. The simplest instance is when the neighbours of a pixel are defined as the pixels whose areas share a common edge with the pixel area in question (direct neighbours). Extensions for this principle are also considered by defining indirect neighbours for a pixel.

Section 3.1 introduces neighbourhoods defined on the square lattice. Because of the simplicity of

their definitions, these neighbourhoods are commonly used for the definition of digital image processing operators. Moreover, it can easily be shown that there exists a one-to-one mapping between the square and the triangular lattice as sketched in Figure 3 below. The hexagonal lattice being of limited practical use for the coarseness of the pixel distribution it induces and the unrealistic aspect of the dual triangular partition.
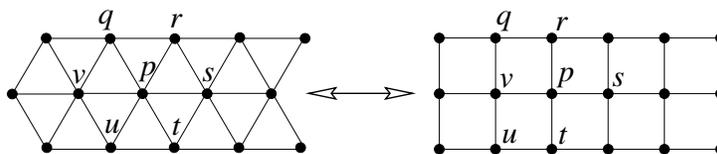

Figure 3: Equivalence between triangular and square lattices.

Building on these definitions, Section 3.2 formally defines digital arcs and connected component which will form the basis for further study. Finally, Section 3.3 sets the basis for the analogy between topological relationships and combinatorial structures.

3.1 Neighbourhoods

Four main neighbourhoods are generally defined on the square lattice. Firstly, the 4-neighbourhood ($N_4(p)$) includes the four direct neighbours of the point in question (see Figure 4(A)). By duality, they are pixel areas which share a common edge with the centre pixel area. This neighbourhood is completed using pixel areas which share a common corner with the pixel area in question (indirect neighbours), leading to the 8-neighbourhood of the point p, $N_8(p)$ (see Figure 4(B)).

By analogy with a chess board, the 8-neighbourhood corresponds to all possible moves of the king. Extending this analogy, the *knight*-neighbourhood ($N_{\text{knight}}(p)$) which corresponds to all possible moves of a knight on the chess board can also be defined (see Figure 4(C)). Finally, the combination of the 8- and the *knight*-neighbourhoods, yields the 16-neighbourhood of p, $N_{16}(p)$ (see Figure 4(D)). Figure 4 illustrates the construction of these neighbourhoods. The lattice is shown as continuous lines whereas dotted lines represent the dual partition. Using this notation, centres of pixels therefore lie at the intersections between continuous (*i.e.*, lattice) lines.
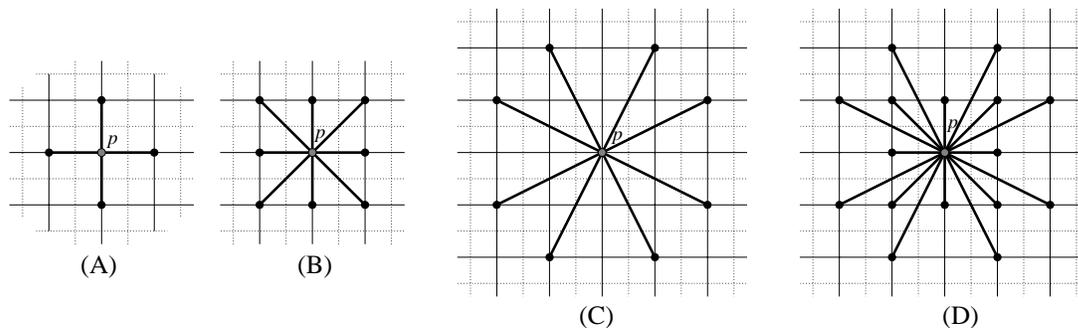

Figure 4: Neighbourhoods on the square grid. (A) $N_4(p)$: 4-neighbourhood. (B) $N_8(p)$: 8-neighbourhood. (C) $N_{\text{knight}}(p)$: *knight*-neighbourhood. (D) $N_{16}(p)$: 16-neighbourhood.

Remark 3.1 *It is important to note that the square lattice is simply a translated version of its dual partition. Moreover, the positions of the points on this lattice are well suited for matrix storage. For these reasons, neighbourhoods on the square lattice are the most well studied and the most commonly used. Rosenfeld [34] defined digital topology on this lattice.*

For later purposes, it is generally the case that codes are associated with moves in the neighbourhood in question. Typically, starting from the positive move along the horizontal axis numbered as 0, moves are sequentially numbered in a counterclockwise fashion as shown in Figure 5.
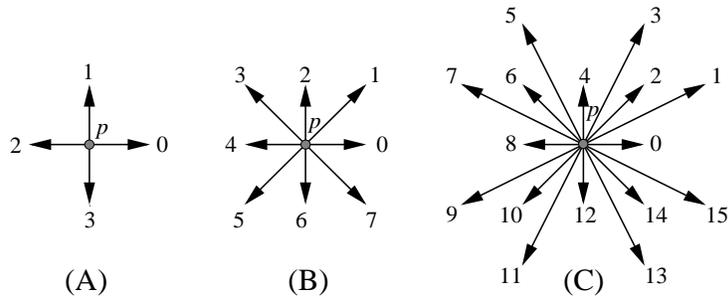
Figure 5: Codes associated with moves on the square grid. (A) 4-neighbourhood. (B) 8-neighbourhood. (C) 16-neighbourhood.

3.2 Digital arcs and closed curves

The concept of neighbourhood allows for the definition of local connectivity between points. Digital arcs and curves are simply an extension of this property. In turn, they impose conditions on their underlying neighbourhoods.

Definition 3.2 *Digital arc.*
Given a set of discrete points with their neighbourhood relationship, a digital arc P_{pq} from the point p to the point q is defined as a set of points $P_{pq} = \{p_i \; ; \; i = 0, \cdots, n\}$ such that:

(i) $p_0 = p$, $p_n = q$.

(ii) $\forall \, i = 1, \cdots, n \Leftrightarrow 1$, p_i has exactly two neighbours in the arc P_{pq}, the points p_{i-1} and p_{i+1}.

(iii) p_0 (respectively p_n) has exactly one neighbour in the arc P_{pq}, namely, point p_1 (respectively p_{n-1}).

Definition 3.3 *Cardinality of a digital arc.*
n is called the cardinality of the digital arc P_{pq} and is also denoted $|P_{pq}|$.

A set of points may satisfy the conditions to be a digital arc using a specific neighbourhood but may not satisfy these conditions for a different neighbourhood. Since most of the definitions and properties depend on the neighbourhood used, we specify this dependence by adding the neighbourhood prefixes (*i.e.*, 4-, 8-, or 16-) to the names of the properties or digital objects cited. For instance, a digital arc in the 16-neighbourhood will be referred to as a 16-arc. Equivalently, a 16-arc is a digital arc with respect to the 16-connectivity relationship.

Using the definition of a digital arc, a connected component on the lattice is defined as follows.

Definition 3.4 *Connected component.*
A connected component on the lattice is a set of points such that there exists an arc joining any pair of points in the set.

A further restriction on connectedness leads to the simple connectivity.

Definition 3.5 *Bounded and simple connected component.*
On the infinite lattice, a connected component that contains an infinite number of points is said to be unbounded. On the finite lattice, a connected component is unbounded if and only if it intersects the border of the lattice. Otherwise, it is said to be bounded.
A simple connected component is a connected component whose complement does not contain any bounded connected component.

By definition a digital arc is a simple connected component.

An important notion in the continuous space is that of closed curves which, in turn, define holes. In the continuous space, Jordan's theorem characterises a closed curve as a curve which partitions the space into two subparts, the interior and the exterior (see *e.g.*, [45]). The definition of a closed curve in the discrete space relies on that of a digital arc.

5

Definition 3.6 *Digital closed curve.*

  A digital closed curve (or equivalently, a digital curve) on the lattice is a set of points such that the removal of one of its points transforms it into a digital arc.

A version of Jordan's theorem in the digital space can be then formulated.

Theorem 3.7 *Discrete Jordan's theorem.*

  A digital curve defines exactly two separate connected components on the lattice, the interior and the exterior. Therefore, there should be no arc joining these two subsets.

Remark 3.8 *Theorem 3.7 emphasises the fact that, by definition, a digital closed curve is not a simple connected component since its interior is bounded (i.e., contains a finite number of points).*

In general, a connectivity relationship cannot be used for both a set and its complement. A duality between possible (k- and k'-) connectivities and neighbourhoods on the lattices is to be defined. We introduce this notion of duality via the following example.

Example 3.9 Dual neighbourhoods on the square lattice.
In Figure 6, the 8-curve C does not separate the digital plane into two 8-components.
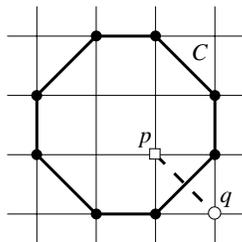

Figure 6: A 8-digital closed curve.

  As counter example, there exist an 8-arc joining two potential interior and exterior points p and q respectively. However, it is clear that an 8-curve will define two 4-connected components as its exterior and interior. Hence, discrete Jordan's theorem will be satisfied when using 8-connectivity (respectively, 4-connectivity) for the curve and 4-connectivity (respectively, 8-connectivity) for the interior and exterior on the square lattice. $\diamond$

Via this duality, the neighbourhood relationships are extended to the connectivity relationships. Therefore, points can now be grouped in different subsets on which operations are to be performed.

Border of a digital set   An important subset of points in digital topology is the set of border points which separates a digital set from its complement.

Definition 3.10 *Border of a digital set.*

  Given a k-connected set of points P, the complement of P, noted P^c, defines a dual connectivity relationship (noted k'-connectivity). In our case, $k = 8$ and $k' = 4$ when using the duality between 8- and 4-connectivities. The border of P is the set of points , defined as the k-connected set of points in P that have at least one k'-neighbour (i.e., a neighbour with respect to the k'-connectivity) in P^c.

An example for this definition can be given when the set of points represents the pixels in a binary image. A binary image is represented by an array of discrete points labelled with a value (1 or 0) which indicates the black or white colour of the corresponding pixels respectively. By convention, two basics subsets can be identified.

Definition 3.11 *Foreground and background in a binary digital image.*

  (i) *The foreground is the set of points F which are labelled with a value equal to 1. By convention, the foreground corresponds to the set of black pixels in a binary image.*

  (ii) *The background is the complement of the set F noted F^c. It is the set of points associated with a zero-value. By convention, the background corresponds to the set of all white pixels in the image.*

6

(iii) The border points are the points that form the border to the set according to Definition 3.10. The corresponding pixels in the image are called border pixels. A point (respectively, a pixel) which is not in the border set is referred to as an interior point (respectively, interior pixel).

Remark 3.12 *The foreground and the background may both contain more than one connected component.*

Example 3.13 Border of a binary digital image.
Consider the digital image shown in Figure 7(A). The black pixels (*i.e.*, points of the foreground F) are symbolised as black circles (●) and the white pixels (*i.e.*, the points of the background F^c) as white circles (○). The 8-connectivity is considered in the foreground F and, hence, the 4-connectivity is considered in the background (*i.e.*, $k = 8$ and $k' = 4$).
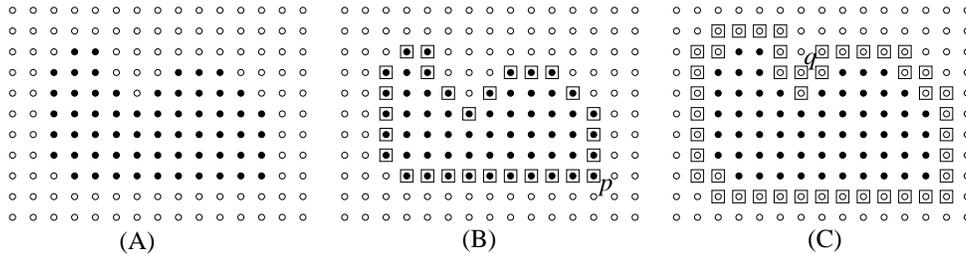

(A)   (B)   (C)

Figure 7: Borders in a binary digital image. (A) The representation of the binary image on the square lattice. (B) The foreground is taken as a closed set. (C) The foreground is taken as a open set.

Depending on which of the foreground or the background is considered as an open set, two different border sets are defined. In Figure 7(B), the foreground is considered as a closed set. Hence, it contains its border. By definition, the border of the foreground is the set of black pixels , that have at least one white pixel among their 4-neighbours. The points in this set are surrounded by a square box in Figure 7(B).

Conversely, in Figure 7(C), the foreground is considered as an open set. The border therefore belongs to its complement, namely the background. In this case, the border is the set , of white pixels that have at least one black pixel among their 8-neighbours. The points in , are surrounded by a square box in Figure 7(C).

From this example, it is clear that the two borders arising from these cases are different.   ◇

Remark 3.14 *Although the set of border points , of a connected component is a connected component with respect to the connectivity of the set it belongs to, it generally does not satisfy the conditions for being a digital closed curve. In the example shown in Figure 7(B), , , the border of the foreground is 8-connected but the point p in the rightmost bottom corner has three 8-neighbours in , . Similarly in Figure 7(C), , is a 4-connected component. However, the point q has three 4-neighbours in , . Therefore, in neither cases is , a closed curve as defined in Definition 3.6.*

Discrete sets are now well characterised in digital topology. The next section introduces the mapping between concepts presented above and terminology given by graph theory. This will allow for creating a favourable context in which a formal study of discrete geometry can be performed.

3.3   Image-to-graph mapping

Earlier work relates image processing and graph theory. Connectivity relationships are mapped onto the graph-theoretical concept of adjacency in the study presented in [28]. Based on this theoretical context, accurate topological thinning can be characterised [30]. Similar results are also developed in [42] where arcs in the connectivity graph are successively deleted to simulate an erosion process. The concept of discrete distance is formulated using graph theory in the early work presented in [23]. Further developments on the study of discrete distances using graph-mapping can be found in [39]. However, in most of these references (with the exception of [39]), the concept of a graph is only used to represent connectivity relationships between pixels. By contrast, we will make use of powerful properties of combinatorial structures and related algorithms for formalising and extending results in discrete spaces.

A graph $G = (V, A)$ is based on the definition of a discrete data set (vertices in V) and their inter-relationship (arcs in A). A digital image is a set of discrete points on which a digital topology can be defined. Moreover, digital topology introduces the concept of neighbourhood for a pixel which, in turn, defines digital arcs and curves.

It is therefore clear that a graph $G = (V, A)$ can be defined using the set of pixels F in the image as set of vertices V. Such a graph is referred to as the grid graph of the image.

Definition 3.15 *[28, 37] Grid graph.*
   Given a set of pixels F in the image and a connectivity relationship on which a digital topology is based, the grid graph $G = (V, A)$ of the image is defined as follows.

   (i) To every pixel p in F corresponds a vertex u in V.

   (ii) An arc (u, v) exists in A whenever the pixels p and q corresponding to vertices u and v respectively are neighbours in the digital topology. The forward star of a given vertex u is the set of vertices v such that arcs (u, v) exist in A. In this study, the forward star of a vertex u corresponds to the set of pixels q in the neighbourhood of the pixel p associated with the vertex u.

   (iii) The length $l(u, v)$ associated with the arc (u, v) is the length of the move made between the corresponding two pixels p and q respectively.

   (iv) The abstract grid graph corresponding to the infinite lattice is called the complete grid graph.

Immediate properties of the grid graph are given in Proposition 3.16.

Proposition 3.16 *By definition of digital topology,*

   (i) The grid graph $G = (V, A)$ of an image is sparse. The number of pixel neighbours to a given pixel is limited by the size of this neighbourhood. Typically, $M_G \leq k.N_G$, where $M_G = |A|$, $N_G = |V|$ and $k = 4$ (4-neighbourhood), 8 (8-neighbourhood) or 16 (16-neighbourhood).

   (ii) The grid graph on a set of N pixels can be constructed in linear time (i.e., in $\mathcal{O}(N)$ operations).

Remark 3.17 *In the previous sections, pixels were identified with discrete points (pixel centres). From now on, a further analogy identifies pixels and vertices in the grid graph. Therefore, pixels will be equivalently referred to as discrete points (e.g., p, q) or vertices (e.g., u, v). Similarly, depending on the context, the set of pixels will be equivalently noted F or V, by analogy with the set of vertices in the grid graph. Finally, arcs in the grid graph will be equivalently referred to as moves on the underlying lattice.*

Definition 3.18 *Path and path length.*
   A path between two vertices u and v in the grid graph $G = (V, A)$ is a set of vertices $P_{uv} = \{u_0, u_1, \ldots, u_n\}$ such that $u_0 = u$, $u_n = v$ and the arc $(u_i, u_{i+1}) \in A$ for any $i = 0, \ldots, n \Leftrightarrow 1$. $n = |P_{uv}|$ is the cardinality of the path P_{uv} and $l(P_{uv}) = \sum_{i=0}^{n-1} l(u_i, u_{i+1})$ is the length of this path.

The notion of connectivity between pixels is mapped onto that of adjacency between vertices in the grid graph. Therefore, the definitions of connected components in digital topology and graph theory are clearly equivalent. Moreover, using this image-to-graph mapping, the concept of the neighbourhood of a pixel is directly mapped onto that of the forward star of a vertex. In the case of a complete grid graph, the forward star of a vertex u readily contains the neighbourhood of the corresponding pixel p (e.g., $N_8(p)$). In the case where the grid graph spans only vertices corresponding to a subset F of pixels in the image (e.g., the foreground pixels in the image), the forward star of a vertex u in such a grid graph will characterise the pixels neighbours to u which are included in F (e.g., $N_8(p) \cap F$).

Example 3.19 Grid graph of the foreground of a binary digital image.
   Consider the binary digital image shown in Figure 8(A). The set F of foreground pixels (i.e., black) is displayed as black circles (•). Empty circles (◦) represent background pixels (i.e., white) in F^c. Figure 8(B) shows the grid graph of the foreground F when considering the 8-neighbourhood relationship (i.e., 8-grid graph). Clearly, this graph is sparse.
   In this example, F is considered as a closed set and therefore border pixels are foreground pixels (i.e., , $\subset F$). By definition of an interior pixel p (i.e., $p \notin$,), all dual neighbours of p are included in F (i.e., $N_4(p) \subset F$ in this case, see Definition 3.10). Therefore, such a pixel p is characterised in the grid graph
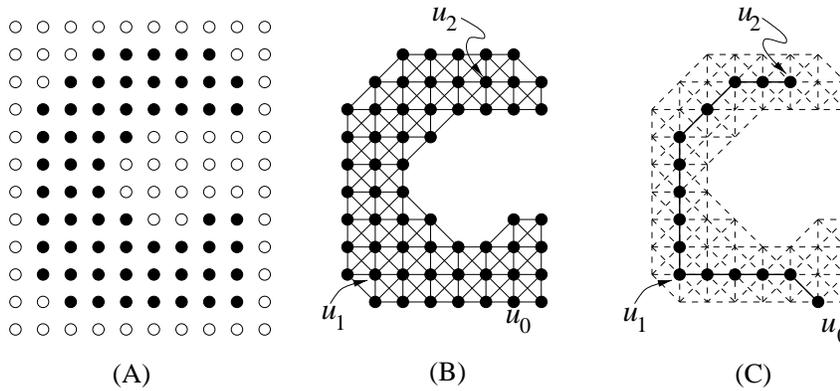
Figure 8: (A) Binary digital image. (B) Corresponding 8-grid graph. (C) A path in the grid graph.

by a vertex whose forward star contains $|N_4(p)| = 4$ vertices corresponding to its 4-neighbouring pixels. For example, this is the case for vertices u_1 and u_2 in Figure 8(B). By opposition, u_0 is a border vertex.

Figure 8(C) shows an example of a path $P_{u_0 u_2}$ between vertices u_0 and u_2 in the grid graph. The analogy between such a path and a digital arc is discussed next. $\diamond$

The mapping between a digital arc and a path in the grid graph needs further precision. A digital arc was defined as a set of neighbouring pixels such that each pixel in the digital arc has exactly two neighbours, except for the start and end vertices (see Definition 3.2). It is therefore clear that a corresponding path in the grid graph is a simple path. However, an additional condition for a simple path in the grid graph to correspond to a digital arc in the image is required. This condition simply states that, for each vertex u in such a path, exactly two vertices in the forward star of u in the graph are included in the path, except for the start and end vertices, each of which has only one adjacent vertex in the path in question. This condition will always be satisfied on any shortest path in a grid graph as discussed in the next section.

For example, in Figure 8(C), $P_{u_0 u_2}$ does not correspond to an 8-digital arc since the predecessor of vertex u_1 has three 8-neighbours on this path. However, it is easy to verify that each sub-path $P_{u_0 u_1}$ and $P_{u_1 u_2}$ defines an 8-digital arc.

4 Discrete geometry

Discrete geometry aims for the characterisation of geometrical properties of a set of discrete points. Geometrical properties of a set are understood to be global properties. Points are grouped, thus forming discrete objects, and it is the properties of these discrete objects that are under study. In contrast, digital topology described in Section 3 allows for the study of the local properties between discrete points within such an object. In short, topological properties such as connectivity and neighbourhood are first used to define discrete objects and discrete geometry then characterises the properties of these discrete objects [5, 35, 45].

4.1 Discrete distance and shortest paths

In this section, we first recall existing definitions and results in discrete geometry applied to the 8-neighbourhood space. Based on the conclusions derived earlier, we aim to map such results in an extended neighbourhood space, the 16-neighbourhood space. Section 4.1.1 introduces the concept of discrete distances. This concept is detailed in relation to the analogy with graph theory, leading to the study of shortest paths in the grid graph in Section 4.1.2. Finally, Section 4.1.3 gives some insights as to the relation between discrete and continuous distances.

4.1.1 Definitions

By analogy with the continuous space, a discrete distance function should verify the classic metric conditions given by Definition 4.1.

Definition 4.1 *Distance.*

Given a set of points P, a function $d : P \times P \to \mathbb{R}^+$ is said to be a distance on P if and only if it satisfies the following conditions.

(i) $d(p,q)$ is defined and finite for all p and q in P (d is total on P).

(ii) $d(p,q) = 0$ if and only if $p = q$ (d is positive definite).

(iii) $d(p,q) = d(q,p)$, $\forall\ (p,q) \in P \times P$ (d is symmetric).

(iv) $d(p,q) + d(q,r) \geq d(p,r)$, $\forall\ (p,q,r) \in P \times P \times P$ (d satisfies the triangular inequality).

In the digital topology, distance calculations are based on local distances within the neighbourhood of a point. Their definitions are related to basic moves on the corresponding lattice as introduced by Definition 4.2.

Definition 4.2 *Move and move length.*

A move on the lattice is the displacement from a point to one of its neighbours. A move length is the value given as local distance between a point and one of its neighbours.

The notion of length for a move can be readily extended to that of a digital arc.

Definition 4.3 *Length of a digital arc.*

The length of a digital arc is the sum of the length of the moves that compose it.

The generic definition for a discrete distance is as follows.

Definition 4.4 *Discrete distance.*

Given the lengths for all possible moves in a neighbourhood, the distance between two points p and q is the length of the shortest digital arc (i.e., the arc of minimal length) from p to q. Although the distance between two points is given as a unique value, the digital arc which realises this distance is not necessarily unique.

The fact that such a distance satisfies the metric conditions relies on the definition of move lengths. Originally, a unit value has been attributed to any move length (e.g., see [36]). In this case, the digital arc associated with the distance between p and q is the arc of minimal cardinality joining p and q. Real or integer move lengths have been designed for a discrete distance related to a specific neighbourhood to achieve a close approximation of the Euclidean distance in the plane [1, 23].

Common definitions of distances are presented here. For each distance, the corresponding discrete disc (Definition 4.5) obtained is also presented. The geometrical properties of such discs constitute an important factor in characterising how close a discrete distance can approximate the Euclidean distance.

Definition 4.5 *Discrete disc.*

Given a discrete distance d_D, a discrete disc of radius $r \geq 0$ centred at point p for this distance is the set of discrete points $\Delta_\mathrm{D}(p,r) = \{q$ such that $d_\mathrm{D}(p,q) \leq r\}$. When no reference to the centre point is necessary, a discrete disc of radius r for the distance d_D will also be noted as $\Delta_\mathrm{D}(r)$.

In the particular case of an infinite square lattice, a point p on the lattice can be uniquely characterised by an integer pair (x_p, y_p) (the coordinates of the point p in the $\mathbb{Z}^2$ plane). Conversely, any integer pair $(x_p, y_p) \in \mathbb{Z}^2$ represents a point p on the square lattice. Therefore, there exists a one-to-one mapping from points on the square lattice to $\mathbb{Z}^2$. This property eases the definition of analytical expressions for the discrete distances on the square lattice.

Definition 4.6 recalls the analytical expression of the Euclidean distance d_E that is used as reference in both continuous and discrete spaces.

Definition 4.6 *Euclidean distance.*

Given two points $p = (x_p, y_p)$ and $q = (x_q, y_q)$ the Euclidean distance value between p and q is given by

$$d_\mathrm{E}(p,q) = \sqrt{(x_q - x_p)^2 + (y_q - y_p)^2}$$

It is easy to verify that d_E satisfies the conditions to be a distance given in Definition 4.1.

All move lengths are first set to unity, leading to the d_4 distance (Definition 4.7) and d_8 distance (Definition 4.9).

Definition 4.7 *City-Block distance.*

The City-Block distance (or Manhattan distance) between p and q is the length of the shortest 4-arc joining p and q when the move lengths are all set to the unity. The City-Block distance between p and q is noted as $d_4(p,q)$ and is also referred to as the d_4 distance.
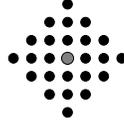
Figure 9: 4-disc of radius 3: $\Delta_4(3)$.

The location of the points on the square lattice allows for an equivalent definition of the d_4 distance.

Proposition 4.8 *Given two points $p = (x_p, y_p)$ and $q = (x_q, y_q)$ on the square lattice, The minimal cardinality of a 4-arc joining p to q is given by:*

$$d_4(p,q) = |x_q \ominus x_p| + |y_q \ominus y_p|$$

As a consequence of Proposition 4.8, the 4-neighbourhood of the point p can be characterised as follows.

$$N_4(p) = \{q = (x_q, y_q) \in \mathbb{Z}^2 \text{ such that } |x_q \ominus x_p| + |y_q \ominus y_p| = 1\} \quad \forall p = (x_p, y_p) \in \mathbb{Z}^2$$

More generally, a discrete 4-disc centred at p and of radius r (*e.g.*, see Figure 9) is characterised by:

$$\Delta_4(p, r) = \{q = (x_q, y_q) \in \mathbb{Z}^2 \text{ such that } |x_q \ominus x_p| + |y_q \ominus y_p| \leq r\}$$

A simple extension of the d_4 distance on the 8-neighbourhood leads to the definition of the Chessboard distance.

Definition 4.9 *Chessboard distance.*

The Chessboard distance (or Diamond distance) between p and q is the length of the shortest 8-arc joining p and q when the move lengths are all set to the unity. The Chessboard distance between p and q is noted as $d_8(p,q)$ and is also referred to as the d_8 distance.
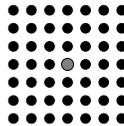
Figure 10: 8-disc centred at p and of radius 3: $\Delta_8(p, 3)$.

Again, using the coordinates of integer points, d_8 can be given an analytical expression as follows.

Proposition 4.10 *Given two points $p = (x_p, y_p)$ and $q = (x_q, y_q)$ on the square lattice, The minimal cardinality of a 8-arc joining p to q is given by:*

$$d_8(p,q) = \max(|x_q \ominus x_p|, |y_q \ominus y_p|)$$

From Proposition 4.10, the 8-neighbourhood of the point p can be characterised as follows.

$$N_8(p) = \{q = (x_q, y_q) \in \mathbb{Z}^2 \text{ such that } \max(|x_q \ominus x_p|, |y_q \ominus y_p|) = 1\} \quad \forall p = (x_p, y_p) \in \mathbb{Z}^2$$

Therefore, an 8-disc of radius r centred at p is also defined by

$$\Delta_8(p, r) = \{q = (x_q, y_q) \in \mathbb{Z}^2 \text{ such that } \max(|x_q \ominus x_p|, |y_q \ominus y_p|) \leq r\}$$

(see Figure 10 for an example). Since the move lengths that define the d_4 and d_8 distances are all equal to 1, both these discrete distance functions satisfy the metric conditions given in Definition 4.1.

Remark 4.11 *Note that there exists a strong similarity between the norms* $\|\vec{u}\|_1 = |x_{\vec{u}}| + |y_{\vec{u}}|$, $\|\vec{u}\|_2 = \sqrt{|x_{\vec{u}}|^2 + |y_{\vec{u}}|^2}$ *and* $\|\vec{u}\|_\infty = \sup(|x_{\vec{u}}|, |y_{\vec{u}}|)$ *defined in the continuous space* $\mathbb{R}^2$ *and* d_4, d_E *and* d_8 *on the digital space. Recalling that* $\|\vec{u}\|_1 \geq \|\vec{u}\|_2 \geq \|\vec{u}\|_\infty \;\forall \vec{u} \in \mathbb{R}^2$, *this property is mapped in the digital space as* $d_4(p,q) \geq d_E(p,q) \geq d_8(p,q) \;\forall p, q \in \mathbb{Z}^2$.

Combining the 8-neighbourhood with the *knight*-neighbourhood, thus forming the 16-neighbourhood with unit move lengths does not yield a distance (see Remark 4.16, later). These neighbourhoods are therefore not detailed further at this stage.

With the aim of improving simplicity and accuracy in the approximation of Euclidean distance on the square lattice, chamfer distances have been introduced as a generalisation of the previous definitions [1, 2]. In chamfer discrete distances, moves are given different lengths depending on some criteria. Chamfer distances have been intensively studied for developing image processing operators.

The generic definition of a chamfer distance is given as follows.

Definition 4.12 *Chamfer distance.*
Given a neighbourhood and associated move lengths the chamfer distance between p *and* q *relative to this neighbourhood is the length of the shortest digital arc from* p *to* q.

A chamfer distance is relative to a neighbourhood associated with move lengths. The cases of further neighbourhoods presented in Section 3.1 are successively detailed.

Starting with the 4-neighbourhood, the length of a 4-move is noted a. In this respect, a 4-move is also called an a-move. Clearly, in the 4-neighbourhood, all moves are equivalent by symmetry or rotation. In this case, the only possible definition of a discrete distance that is geometrically consistent is that of the d_4 distance, where $a = 1$.

A simple extension of the 4-neighbourhood leads to the 8-neighbourhood. Diagonal moves are added to the horizontal and vertical moves. The length of such diagonal moves is noted b. In this respect, diagonal moves are called b-moves and the chamfer distance obtained in the 8-neighbourhood is noted $d_{a,b}$. Given any positive value for a (*i.e.*, the length for all 4-moves), in order to preserve a geometrical consistency within the 8-neighbourhood, the diagonal moves should be associated with a length b larger than a. In this context, the most natural value is $b = a\sqrt{2}$, since it allows for an exact value of the chamfer distance along the diagonal lines from a given point. However, for the sake of simplicity of computation and storage, it is also important to preserve integer arithmetic for distance calculations. In this respect, integer values for a and b have been derived (*e.g.*, see [1, 2, 14, 23]). The most commonly used set of such values is ($a = 3$, $b = 4$) [1, 2].

Referring to Section 3.1, a further extension defines the 16-neighbourhood. The *knight*-move is introduced and its length is noted c (thus defining a c-move). The chamfer distance obtained in the 16-neighbourhood is noted $d_{a,b,c}$. Assuming that $a = 1$, $b = \sqrt{2}$, the value $c = \sqrt{5}$ allows for an exact chamfer distance value along the lines that support the c-moves. For preserving integer calculations of chamfer distances, the lengths of the moves included in the 16-neighbourhood $(1, \sqrt{2}, \sqrt{5})$ are commonly approximated by using the set of integer values ($a = 5$, $b = 7$, $c = 11$) [1, 2].

The fact that a chamfer distance satisfies the metric conditions given in Definition 4.1 depends on the values of the move lengths. Hence, restrictions on these values for chamfer distances to satisfy the metric conditions have been set.

Proposition 4.13 *The conditions on* a *and* b *for* $d_{a,b}$ *to be a discrete distance are*

$$0 < a \leq b \leq 2a$$

The typical values $a = 3$ and $b = 4$ satisfy these conditions and therefore $d_{3,4}$ is a distance in the 8-neighbourhood. In this case, the value of the diagonal move length $\sqrt{2}$ is approximated by $\frac{4}{3}$.

Remark 4.14 *Note that the values* $a = b = 1$ *used for the definition of* d_8 *satisfy the conditions given in Proposition 4.13. Therefore,* d_4 *and* d_8 *can be seen as particular cases of chamfer distances in the 4- and 8-neighbourhoods respectively.*

Similar conditions can be expressed in the 16-neighbourhood for $d_{a,b,c}$ to be a discrete distance.

Proposition 4.15 *The values of a, b and c should satisfy the following conditions for $d_{a,b,c}$ to be a distance on the 16-neighbourhood.*

$$0 < a \leq b \leq 2a \leq c \; and \; c \leq a + b \; and \; 3b \leq 2c$$

Again, the typical values for the move lengths $a = 5$, $b = 7$ and $c = 11$ satisfy the above conditions. Therefore, $d_{5,7,11}$ is a distance. In this case, the diagonal move length $\sqrt{2}$ is approximated by $\frac{b}{a} = \frac{7}{5}$ and the *knight*-move length of $\sqrt{5}$ is approximated by $\frac{c}{a} = \frac{11}{5}$.

Remark 4.16 *The values $a = b = c = 1$ do not satisfy the conditions given in Proposition 4.15. Therefore, as mentioned earlier, an extension of d_8 in the 16-neighbourhood by setting all move lengths to unity is not possible.*

Chamfer discs are presented in Figure 11. Typically, the convex hull of a chamfer disc in the 8-neighbourhood is an octagon that approximates the Euclidean circle depending on the values of a and b. More generally, a chamfer disc is a polygon with as many sides as there are different moves in the neighbourhood on which the chamfer distance is defined.
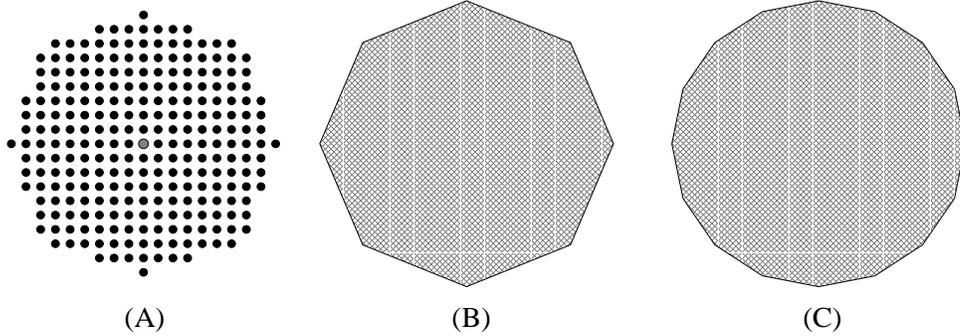

Figure 11: Chamfer discs. (A) $\Delta_{3,4}(27)$. (B) $\Delta_{a,b}$. (C) $\Delta_{a,b,c}$.

The definition of chamfer distances readily suggests further extensions of the neighbourhoods. This procedure makes use of Farey sequences to define extra basic moves (*e.g.*, see [23]). Conditions on the lengths of these moves can be developed analytically [43].

By analogy with the definition of a discrete distance, it is clear that the discrete distance value between two pixels is the length of the shortest path between the two corresponding vertices in the grid graph [13, 23, 24, 25, 39]. Moreover, the properties of the shortest path justify the fact that such a length defines a distance. The definition of grid graph allows for the use of shortest path algorithms since it is a sparse graph with typically small positive arc lengths (see Proposition 3.16). Finally, using such an approach one can take advantage of by-products arising from such algorithms.

Definition 4.17 *Shortest path base graph.*
Given the grid graph $G = (V, A)$ with arc lengths and two vertices $u \in V$ and $v \in V$, the shortest path base graph associated with the vertices u and v is the subgraph $\mathrm{SPBG}(u, v)$ of G formed by all possible shortest paths from u to v. The notation for the shortest path base graph will include the dependency of the neighbourhood relationship considered with an index k (i.e., SPBG_k) corresponding to that neighbourhood space (e.g., $k = 4, 8, 16$).

Typical properties of a shortest path base graph in the 8-neighbourhood space are given in Example 4.18.

Example 4.18 Shortest path base graph in the 8-neighbourhood space (SPBG_8).
Consider the complete 8-grid graph $G = (V, A)$ presented in Figure 12(A). Given the two vertices $u \in V$ and $v \in V$, the shortest path base graph $\mathrm{SPBG}_8(u, v)$ is shown as bold lines in Figure 12(B).

Montanari [23] has proved that there exists a shortest path in the complete 8-grid graph between any two vertices $u, v \in V$ that consists of only two straight segments, one horizontal (or vertical) and one diagonal. It is therefore clear that any shortest path in the complete 8-grid graph will be composed of at most two basic directions. Hence, the shortest path base graph $\mathrm{SPBG}_8(u, v)$ is included in a parallelogram shape, as shown in Figure 12(B). $\diamond$
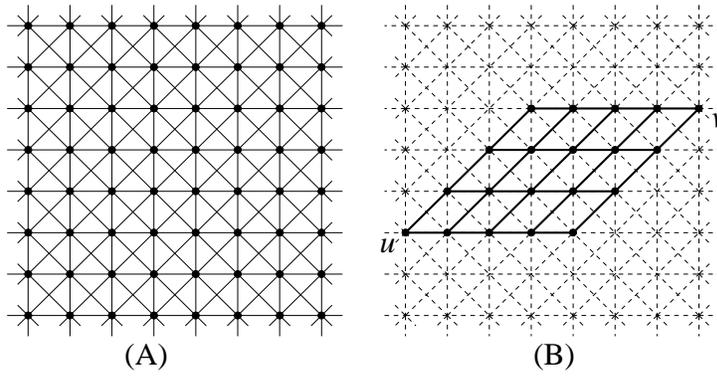
13

Figure 12: (A) 8-neighbourhood complete grid graph. (B) Shortest path base graph $SPBG_8(u, v)$.

Definition 4.19 *Number of moves in a path.*

In the 8-grid graph, arcs correspond to either a- or b-moves. In this respect, given an 8-path P_{uv} between two vertices u and v, $k_a(u, v)$ (respectively $k_b(u, v)$) denotes the number of arcs corresponding to a-moves (respectively b-moves) in P_{uv}. The length of P_{uv} is therefore given by $l(P_{uv}) = a.k_a(u, v) + b.k_b(u, v)$.

Similarly, in the 16-grid graph, the length of a 16-path P_{uv} is given by $l(P_{uv}) = a.k_a(u, v) + b.k_b(u, v) + c.k_c(u, v)$, where $k_c(u, v)$ is the number of arcs corresponding to c-moves in P_{uv}.

The 8-grid graph considered now is that shown in Figure 8 and described in Example 3.19. In contrast with a complete grid graph, it is the grid graph of a bounded connected component. Figure 13(A) shows the shortest path spanning tree rooted at u_0 obtained with arc lengths $a = 3$ and $b = 4$.
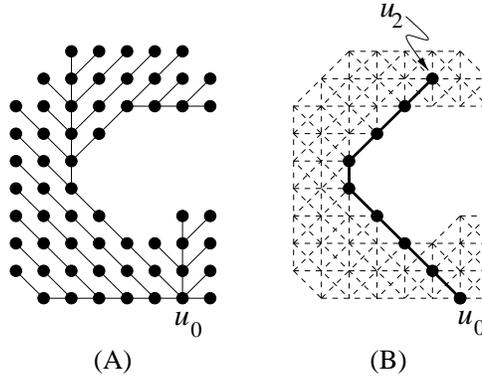

Figure 13: (A) Shortest path spanning tree in the grid graph shown in Figure 8(A). (B) An example of shortest path.

In such an 8-grid graph, the previous description of a shortest path is not always valid since the shortest path between two vertices may be constrained by the border of the component. Figure 13(B) shows such a shortest path of length $l(P_{u_0 u_2}) = 31$ between u_0 and u_2. Clearly, this shortest path in the grid graph corresponds to an 8-digital arc. Moreover, it is the only possible shortest path between u_0 and u_2 in the grid graph.

We now take a closer look at shortest paths in the 16-neighbourhood space. Our aim is to highlight the advantages of this neighbourhood in some applications compared to the 8-neighbourhood commonly used. Shortest paths are first characterised and their properties further detailed. Results concerning the comparison of shortest path lengths and cardinalities in the 8- and 16-neighbourhood spaces are developed in Section 4.1.2 to emphasise the need for such a study.

Given two vertices u and v, we define $SP_{16}(u, v)$ as the 16-shortest path between these two vertices. Let (x_u, y_u) and (x_v, y_v) be the coordinates of the vertices u and v in the real plane. The origin is arbitrary. The 16-shortest path $SP_{16}(u, v)$ can be defined by the respective number of moves taken in

the three directions on the grid graph. Let $k_a(u,v)$, $k_b(u,v)$ and $k_c(u,v)$ be the composition of arcs corresponding to a-moves, b-moves and c-moves respectively on the 16-shortest path from u to v.
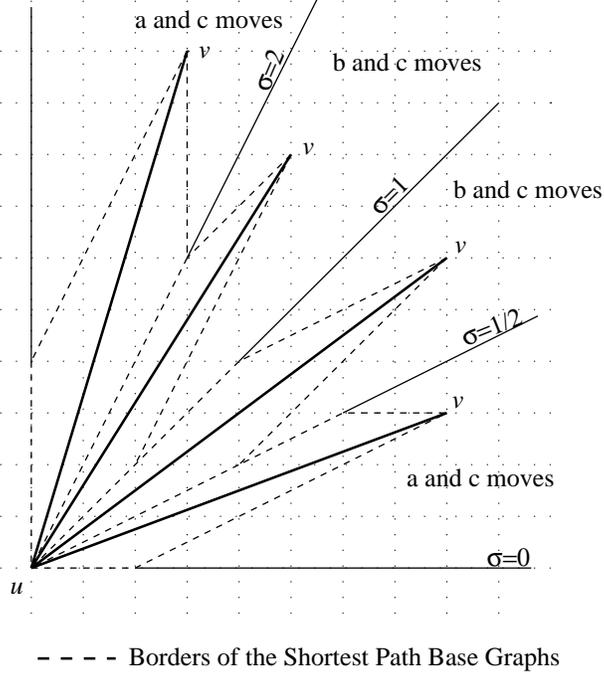

- - - - Borders of the Shortest Path Base Graphs

Figure 14: Illustration of the shortest paths in the first quadrant of $\mathbb{R}^2$.

Proposition 4.20 $SP_{16}(u,v)$ *is composed of arcs corresponding to, at most, two types of moves.*

Proof:
Given two vertices u and v, let σ be the slope of $[p,q]$. Without loss of generality, we only consider the case of the first octant ($0 \leq \sigma \leq 1$) as shown in Figure 14.

- $\sigma = 0$: $k_a(u,v) = |x_v - x_u|$; $k_b(u,v) = 0$; $k_c(u,v) = 0$

- $0 < \sigma < \frac{1}{2}$: $|x_v - x_u| > 2|y_v - y_u|$ then:

$$k_c(u,v) = |y_v - y_u| \quad ; \quad k_a(u,v) = |x_v - x_u| - 2k_c(u,v) \quad ; \quad k_b(u,v) = 0$$

- $\sigma = \frac{1}{2}$: $k_a(u,v) = 0$; $k_b(u,v) = 0$; $k_c(u,v) = |y_v - y_u|$

- $\frac{1}{2} < \sigma < 1$: $2|y_v - y_u| > |x_v - x_u| > |y_v - y_u|$ then:

$$k_c(u,v) = |x_v - x_u| - |y_v - y_u| \quad ; \quad k_b(u,v) = |y_v - y_u| - k_c(u,v) \quad ; \quad k_a(u,v) = 0$$

- $\sigma = 1$: $k_a(u,v) = 0$; $k_b(u,v) = |x_v - x_u|$; $k_c(u,v) = 0$

The other cases are equivalent by symmetry. □

Proposition 4.20 can be seen as an extension of the Montanari's characterisation of (8-)shortest path [23]. More specifically, the possible combinations of moves on $SP_{16}(u,v)$ are: a, b or c-moves occurring singly, a and c-moves, or b and c-moves. The combination a and b-moves never occurs since the condition $a + b \geq c$ has to be satisfied.

The shortest path base graph $SPBG_{16}(u,v)$ is the sub-graph formed by of all possible 16-shortest paths from u to v. An example is given in Figure 15, where the two moves are a and c.
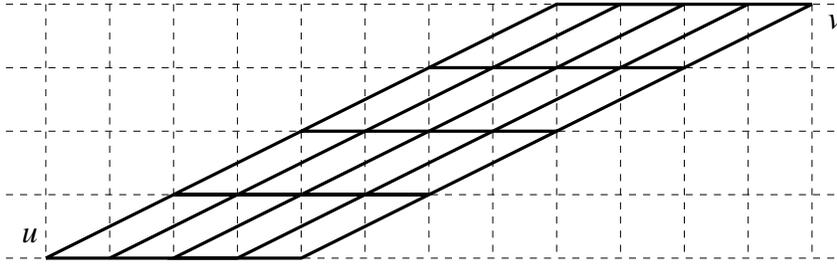
Figure 15: Shortest path base graph $\mathrm{SPBG}_{16}(u,v)$.

4.1.2 Shortest path cardinality

In this section, we compare the cardinality of the 16-shortest path SP_{16} using $d_{a,b,c}$ with that of the 8-shortest path SP_8 using $d_{a,b}$. We assume that the values of a and b are the same for the 8-neighbourhood and the 16-neighbourhood, and that a, b and c satisfy the conditions defined in the previous sections. Throughout, we take V to be the set of all pixels on the unit square grid.

Proposition 4.21 $|\mathrm{SP}_{16}(u,v)| \le |\mathrm{SP}_8(p,q)| \quad \forall u,v \in V$.

Proof:
Without loss of generality, we only consider the case of the first octant $(0 \le \sigma \le 1)$.
  If:

- $\sigma = 0,1$:
  $$|\mathrm{SP}_{16}(u,v)| = |\mathrm{SP}_8(u,v)| = \max(|x_u - x_v|, |y_v - y_u|)$$

- $\sigma = \frac{1}{2}$:
  $$|\mathrm{SP}_{16}(u,v)| = \min(|x_v - x_u|, |y_v - y_u|)$$
  Now, $\min(|x_v - x_u|, |y_v - y_u|) < \max(|x_v - x_u|, |y_v - y_u|)$
  And, $\max(|x_v - x_u|, |y_v - y_u|) = |\mathrm{SP}_8(u,v)|$

- $0 < \sigma < \frac{1}{2}$: $|\mathrm{SP}_{16}(u,v)| = |x_v - x_u| - |y_v - y_u|$
  Now $|x_v - x_u| - |y_v - y_u| < |x_v - x_u|$
  And, $|x_v - x_u| = |\mathrm{SP}_8(u,v)|$

- $\frac{1}{2} < \sigma < 1$:
  $$|\mathrm{SP}_{16}(u,v)| = 2|y_v - y_u| - |x_v - x_u|$$
  Now, $2|y_v - y_u| - |x_v - x_u| < 2|x_v - x_u| - |x_v - x_u|$
  And, $2|x_v - x_u| - |x_v - x_u| = |x_v - x_u| = |\mathrm{SP}_8(u,v)|$

$\square$

  Therefore, the storage of a 16-shortest path between two pixels p and q can be, at worst, equal to that of a 8-shortest path $(\sigma \in \{-1,0,1,\infty\})$ and, at best, half that of the 8-shortest path $(\sigma \in \{-\frac{1}{2}, \frac{1}{2}\})$.

  We have a similar proposition regarding the length of the shortest path as that of its cardinality.

Proposition 4.22 $l(\mathrm{SP}_{16}(u,v)) \le l(\mathrm{SP}_8(u,v) \quad \forall u,v \in V$.

Proof :
  We only consider the case of the first octant $(0 \le \sigma \le 1)$.

- $\sigma = 0,1 : l(\mathrm{SP}_8(u,v)) = l(\mathrm{SP}_{16}(u,v)) = a.k_{\mathrm{a}}(u,v) + b.k_{\mathrm{b}}(u,v)$

16

- $\sigma = \frac{1}{2}$:

    $l(\mathrm{SP}_{16}(u,v)) = c.|y_v - y_u|$

    $l(\mathrm{SP}_8(u,v)) = a.(|x_v - x_u| - |y_v - y_u|) + b.|y_v - y_u|$

    Since, $|x_v - x_u| = 2|y_v - y_u|$ then, $l(\mathrm{SP}_8(u,v)) = (a+b).|y_v - y_u|$

    Also since, $a+b \geq c$ then, $l(\mathrm{SP}_8(u,v)) \geq c.|y_v - y_u| = l(\mathrm{SP}_{16}(u,v))$

- $0 < \sigma < \frac{1}{2}$:

    $l(\mathrm{SP}_{16}(u,v)) = c.|y_v - y_u| + (|x_v - x_u| - 2|y_v - y_u|).a$

    $l(\mathrm{SP}_8(u,v)) = a.(|x_v - x_u| - |y_v - y_u|) + b.|y_v - y_u|$

    $l(\mathrm{SP}_8(u,v)) - l(\mathrm{SP}_{16}(u,v)) = (b + a - c).|y_v - y_u|$

    Since, $a+b \geq c$ then, $l(\mathrm{SP}_8(u,v)) - l(\mathrm{SP}_{16}(u,v)) \geq 0 \Rightarrow l(\mathrm{SP}_8(u,v)) \geq l(\mathrm{SP}_{16}(u,v))$

- $\frac{1}{2} < \sigma < 1$:

    $l(\mathrm{SP}_{16}(u,v)) = c.(|x_v - x_u| + |y_v - y_u|) + b.(2|y_v - y_u| - |x_v - x_u|)$

    $l(\mathrm{SP}_8(u,v)) = a.(|x_v - x_u| - |y_v - y_u|) + b.|y_v - y_u|$

    $l(\mathrm{SP}_8(u,v)) - l(\mathrm{SP}_{16}(u,v)) = (b + a - c).(|y_v - y_u| - |x_v - x_u|)$

    Since, $a+b \geq c$ then, $l(\mathrm{SP}_8(u,v)) - l(\mathrm{SP}_{16}(u,v)) \geq 0 \Rightarrow l(\mathrm{SP}_8(u,v)) \geq l(\mathrm{SP}_{16}(u,v))$

$\qquad\qquad\qquad\qquad\qquad\qquad\qquad\qquad\qquad\qquad\qquad\qquad\qquad\qquad\qquad\qquad\quad\square$

Remark 4.23 *The need for the condition $a+b \geq c$ is emphasised by the above result.*

The above result highlights the performance of discrete distances based on the 16-neighbourhood for the approximation of Euclidean distances. The addition of the *knight*-move allows for more flexibility and therefore more precision when approximating real distances. Moreover, the relation between discrete distances in the extended neighbourhood and Euclidean distances is given in the next section.

4.1.3 Relation with Euclidean distance

Given $k_a(u,v)$, $k_b(u,v)$ and $k_c(u,v)$ on the 16-shortest path between u and v, the Euclidean distance between u and v is given by the following proposition.

Proposition 4.24

$$d_\mathrm{E}(u,v) = \sqrt{(k_a(u,v) + k_b(u,v) + 2k_c(u,v))^2 + (k_b(u,v) + k_c(u,v))^2} \quad \forall u,v \in V$$

Proof:
With the aid of Figure 14, we consider the following cases for $0 \leq \sigma \leq 1$:

- $\sigma = 0$: $d_\mathrm{E}(u,v) = k_a(u,v), \quad k_b(u,v) = 0, \, k_c(u,v) = 0$

- $0 < \sigma < \frac{1}{2}$: $d_\mathrm{E}(u,v) = \sqrt{(k_a(u,v) + 2k_c(u,v))^2 + k_c(u,v)^2}, \quad k_b(u,v) = 0$

- $\sigma = \frac{1}{2}$: $d_\mathrm{E}(u,v) = \sqrt{4k_c(u,v)^2 + k_c(u,v)^2}, \quad k_a(u,v) = 0, \, k_b(u,v) = 0$

- $\frac{1}{2} < \sigma < 1$: $d_\mathrm{E}(u,v) = \sqrt{(k_b(u,v) + 2k_c(u,v))^2 + (k_b(u,v) + k_c(u,v))^2}, \quad k_a(u,v) = 0$

- $\sigma = 1$: $d_\mathrm{E}(u,v) = \sqrt{k_b(u,v)^2 + k_b(u,v)^2}, \quad k_a(u,v) = 0, \, k_c(u,v) = 0$

The other cases are equivalent by symmetry. Therefore, Proposition 4.24 holds. $\qquad\square$

Remark 4.25 *A similar formula is readily obtained for the case of the 8-neighbourhood space. In this case,*

$$d_\mathrm{E}(u,v) = \sqrt{(k_a(u,v) + k_b(u,v))^2 + k_b(u,v)^2} \quad \forall u,v \in V$$

Such a result allows for further developments for characterising analytically errors made when using discrete distances compared to continuous distances (see *e.g.*, [22]). As a by-product, they allow for the characterisation of optimal values of move lengths (*e.g.*, a, b, c) regarding this criterion.

4.2 Discrete convexity

Results presented in this section summarise the development of definitions and characterisation of discrete convexity. Most of these results are presented in great detail in references [3, 16, 17, 18, 19, 27, 31, 32]. We adopt the notation in reference [27] for introducing discrete convexity.

Definition 4.26 *Notation for discrete convexity.*

- *Given a set of discrete points P, the cardinality of P is the number of discrete points that is included in P and is noted $|P|$.*

- *Given a set of discrete points $P = \{p_i\}$, $<P>$ is the set of discrete points contained in $[P]$, the continuous convex hull of P.*

- *If P contains a finite number of discrete points (i.e., $n = |P|$ is finite), then, P can be written as $P = \{p_0, p_1, \ldots, p_n\}$. In this case, $<P>$ can be equivalently written as $<p_0, p_1, \ldots, p_n>$.*

A continuous set S is convex if and only if $[S] = S$. A similar characterisation of discrete convexity via the continuous convex hull of P can be formulated as follows.

Proposition 4.27 *[3, 16, 18] A set of discrete points P is discrete convex if and only if any discrete point contained in the convex hull of P belongs to P. In short, P is discrete convex if and only if $<P>= P$.*

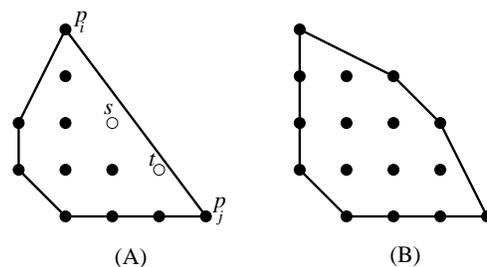Figures 16(A) and 16(B) display the resulting characterisation of discrete convexity. Moreover, Proposi-

Figure 16: A characterisation of discrete convexity.

tion 4.27 holds if and only if for any discrete points p, q and r in P, $<p, q, r>\subseteq P$ (see [27]). For a set of discrete points, such a property is called triangle-convexity (T-convexity) [27]. Different alternative characterisations of discrete convexity exist. Under certain conditions (mostly simple connectivity), they can be proved to be equivalent one to another. Figure 17 gives a summary of such developments.
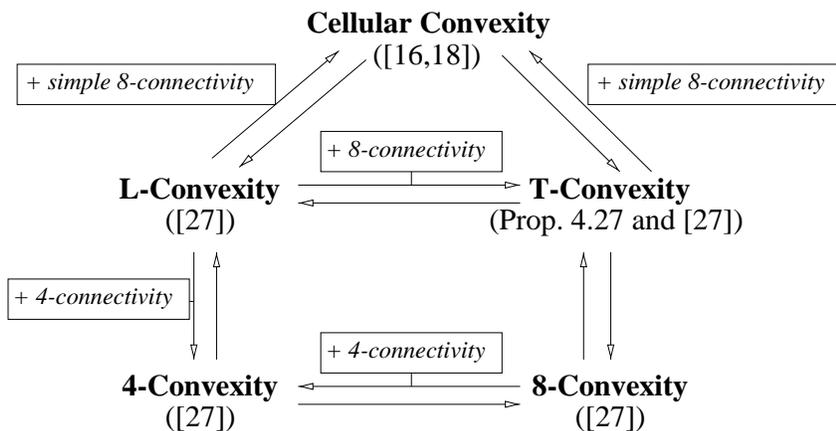

Figure 17: Equivalence between characterisations of discrete convexity.

A geometrical characterisation of discrete convexity similar to that of continuous convexity can now be formulated.

Proposition 4.28 *[18] A set of discrete points P is discrete convex if and only if any point $p_i \in P$ is connected to any other point $p_j \in P$ by an 8-digital straight segment whose points belong to P.*

Such a characterisation gives a first insight as to the definition of discrete straightness. When applied to digital arcs, Proposition 4.28 reduces to the following.

Proposition 4.29 *[18] A digital arc is a digital straight segment if and only if it is discrete convex.*

Section 4.3 will detail a formal characterisation of discrete straightness. In Section 5, we aim to extend these results to the 16-neighbourhood space.

4.3 Discrete straightness

In the discrete space, straightness is referred to as discrete straightness. The following introductory definition for this concept is given.

Definition 4.30 *Digital straight segment.*
A discrete set of points is a digital straight segment if it is the digitisation of at least one continuous straight segment.

Definition 4.30 only takes its full meaning when the digitisation scheme is defined. The most commonly used digitisation scheme is the grid-intersect quantisation [10] and is presented here through the following example.

Consider the continuous segment $[\alpha, \beta]$ and the square lattice shown in Figure 18. The intersection points between $[\alpha, \beta]$ and the lattice lines are mapped to their nearest integer points. In case of a tie, the discrete point which is locally at the right of $[\alpha, \beta]$ is selected ($[\alpha, \beta]$ is oriented from α to β). This digitisation scheme is illustrated in Figure 18 by the fact that intersections between $[\alpha, \beta]$ and lattice lines are mapped their closest discrete points on the lattice.
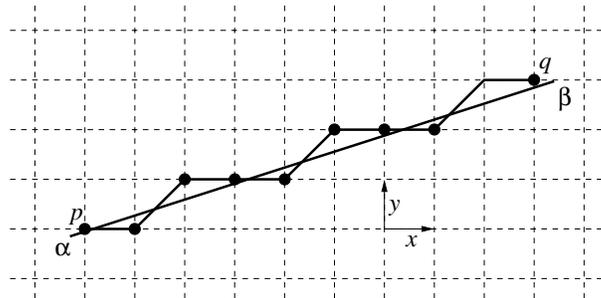

Figure 18: Grid-intersect quantisation.

The set of discrete points $\{p_i\}_{i=0\cdots n}$ resulting from the digitisation of a continuous segment $[\alpha, \beta]$ is called the digitisation set of $[\alpha, \beta]$. It can then be shown that the grid-intersect quantisation of a continuous straight segment is an 8-digital arc [33].

Different approaches have been taken to characterise discrete straightness in the 8-neighbourhood space. Clearly, the minimum requirement for a set of discrete points to form an digital straight segment is that this set forms a digital arc defined by Definition 3.2.

4.3.1 Freeman's codes

The first characterisation of a digital straight segment has been given by Freeman [10, 11]. This characterisation is descriptive and makes use of codes that are defined for all possible moves in the 8-neighbourhood (see Section 3.1). The particular structure of a sequence of such codes (*i.e.*, the chain-code) is then used to characterise discrete straightness (Proposition 4.33).

Definition 4.31 *Freeman's codes and chain-code.*
All possible moves in the 8-neighbourhood are numbered successively counterclockwise from 0 to 7, as shown in Figure 19.

The encoding $\{c_i\}_{i=1,\cdots n}$ ($c_i \in \{0, 1, \ldots, 7\}$) of a given sequence of 8-moves defined by the discrete points $\{p_i\}_{i=0,\cdots n}$ is called the chain-code of this sequence.
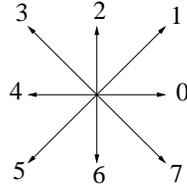

Figure 19: Freeman's codes in the 8-neighbourhood.

Example 4.32 Chain-code.
The chain-code of the 8-move sequence depicted in Figure 20 is

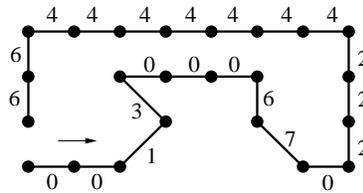$$\{0, 0, 1, 3, 0, 0, 0, 6, 7, 0, 2, 2, 2, 4, 4, 4, 4, 4, 4, 4, 6, 6\}$$

$\diamond$

Figure 20: An example of the use of Freeman's code.

The characterisation of a digital straight segment using the chain-code is formulated as in Proposition 4.33. Note that, since the grid-intersect quantisation of a continuous straight segment in an 8-digital arc, Proposition 4.33 below assumes that the 8-move sequence considered forms an 8-digital arc.

Proposition 4.33 *An 8-digital arc is a digital straight segment if and only if its chain-code satisfies the following conditions [10]:*

(i) At most two types of codes can be present, and these can differ only by unity, modulo eight.

(ii) One of the two code values always occurs singly.

(iii) Successive occurrences of the code occurring singly are as uniformly spaced as possible.

Algorithms that test for the straightness of a digital arc can be derived from adapted versions of this proposition. They are based on different rules derived from the conditions given in Proposition 4.33 (*e.g.*, [10, 15, 33]).

4.3.2 Chord properties

This section introduces a different class of characterisation for discrete straightness called *chord properties*. Originally proposed by Rosenfeld [33], the chord property (Proposition 4.34) remains one of the major results in discrete geometry. Variations and generalisations of the original characterisation have been proposed and are also detailed in this section.
Proposition 4.34 first introduces the chord property as originally formulated in [33].

Proposition 4.34 *[33] An 8-digital arc $P_{pq} = \{p_i\}_{i=0\cdots n}$ satisfies the chord property if and only if, for any two discrete points p_i and p_j in P_{pq} and for any real point α on the continuous segment $[p_i, p_j]$, there exists a discrete point $p_k \in P_{pq}$ such that $d_8(\alpha, p_k) < 1$.*
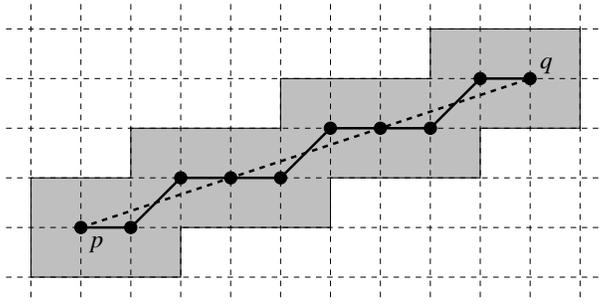
Figure 21: Example of the validity of the chord property.

Remark 4.35 *In Proposition 4.34, the definition of the (Chessboard) d_8 distance is extended to real points via its analytical characterisation given by Proposition 4.10 (i.e., $d_8(\alpha, \beta) = \max(|x_\beta \Leftrightarrow x_\alpha|, |y_\beta \Leftrightarrow y_\alpha|)$ for any $\alpha = (x_\alpha, y_\alpha)$ and $\beta = (x_\beta, y_\beta)$ in $\mathbb{R}^2$).*

Geometrically, the chord property and the resulting visibility polygon can be illustrated by Figure 21.

Given the digital arc P_{pq}, the shaded polygon in Figure 21 illustrates the set of points $\alpha \in \mathbb{R}^2$ such that there exists a discrete point $p_k \in P_{pq}$ such that $d_8(\alpha, p_k) < 1$ (i.e., the visibility polygon is the union of 8-discs of unit radii centred at every discrete point p_k of P_{pq}). From Proposition 4.34, P_{pq} satisfies the chord property if and only if the continuous segment $[p_i, p_j]$ is totally contained in this area for any i and j in $\{0, \ldots, n\}$. The chord property can therefore be reformulated as follows: "An 8-digital arc $P_{pq} = \{p_i\}_{i=0 \ldots n}$ satisfies the chord property if and only if any point p_i is visible from any other point p_j within the visibility polygon defined by $\{\alpha \in \mathbb{R}^2$ such that $d_8(p_k, \alpha) < 1$ for all $k = 0, \ldots, n\}$".
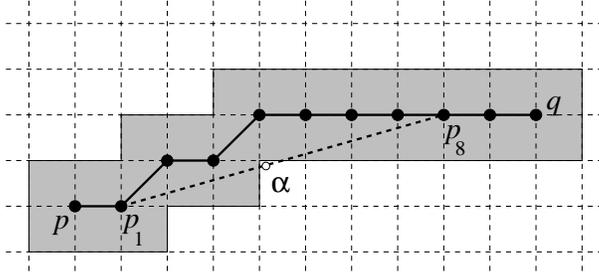

Figure 22: Example for the violation of the chord property.

Figure 22 illustrates an instance where the conditions for the chord property are not satisfied. In this example, it is clear that $\alpha \in [p_1, p_8]$ is such that $d_8(p_k, \alpha) \geq 1$ for any $k = 0, \ldots, n$. In other words, α is outside the visibility polygon and p_1 is not visible from p_8 (and conversely) within the visibility polygon.

Remark 4.36 *If P_{pq} does not satisfy the chord property, then there exist two points p_i and p_j in P_{pq} such that $[p_i, p_j]$ intersects the visibility polygon associated with P_{pq} in a single point r (i.e., there exists $p_k \in P_{pq}$ such that $d_8(p_k, r) = 1$). In this case, r is an integer point. This property is illustrated in Figure 23, where P_{pq} is the same digital arc as in Figure 22, $i = 1$, $j = 7$ and $k = 3$ or $k = 4$.*

The chord property is an essential result since it gives an analytical formulation of discrete straightness via Theorem 4.37 below.

Theorem 4.37 *[33] In the 8-digital space:*

(i) The digitisation of a straight line is a digital arc and has the chord property.

(ii) If a digital arc has the chord property, it is the digitisation of a straight line segment.

The original proof of Theorem 4.37 can be found in [33]. A simpler proof based on Santaló's theorem is given in [29].
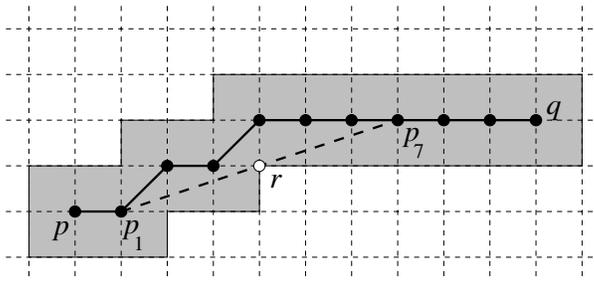
Figure 23: A special case for the violation of the chord property.

This result enables one to test the discrete straightness of an 8-digital arc without reference to any related continuous segment whose digitisation would yield the digital arc in question. Moreover, the concept of visibility is important since it readily suggests a simple greedy algorithm which would successively test for the visibility of a point from other points in the digital arc under study (see Section 6).

Areas of visibility polygons defined in Proposition 4.34 are clearly not minimal. By definition, this polygon should be convex. The compact chord property aims for the reduction of visibility polygons by using the d_4 distance.

Proposition 4.38 *[40] An 8-digital arc $P_{pq} = \{p_i\}_{i=0\cdots n}$ satisfies the compact chord property if and only if, for any two distinct discrete points p_i and p_j in P_{pq} and for any real point α on the continuous segment $[p_i, p_j]$, there exists a real point $\beta \in \mathbb{R}^2$ in the broken line $\bigcup_i [p_i, p_{i+1}]$ such that $d_4(\alpha, \beta) < 1$.*

Remark 4.39 *In Proposition 4.38, the definition of the d_4 distance is extended to real points via its analytical characterisation given by Proposition 4.8 (i.e., $d_4(\alpha, \beta) = |x_\beta \Leftrightarrow x_\alpha| + |y_\beta \Leftrightarrow y_\alpha|$ for all $\alpha = (x_\alpha, y_\alpha)$ and $\beta = (x_\beta, y_\beta)$ in $\mathbb{R}^2$).*

The visibility polygon defined in the compact chord property is the set $\{\alpha \in \mathbb{R}^2$ such that $d_4(\beta, \alpha) < 1\}$ where $\beta \in \mathbb{R}^2$ is on the continuous segment $[p_i, p_j]$ for all $i, j = 0, \ldots, n$. It therefore corresponds to a unit 4-disc swept along the broken line $\bigcup_i [p_i, p_{i+1}]$. Figure 24 illustrates the difference between visibility polygons induced by the chord and compact chord properties respectively. The shaded polygon is the visibility polygon defined by the compact chord property (Proposition 4.38), whereas the dashed bold polygon represents the contour of the visibility polygon defined by the chord property (Proposition 4.34). Since one is always included in the other, the term "compact chord property" was used.

Figure 24: Example for the validity of the compact chord property.
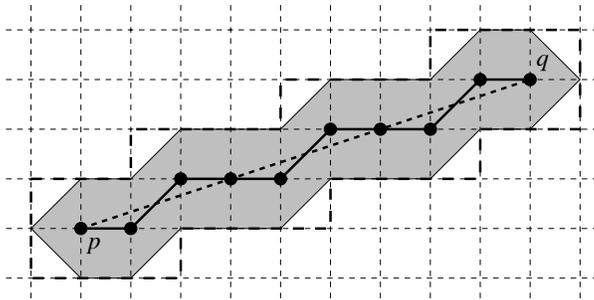
Using the same example as in Figure 22, Figure 25 shows that the digital arc also fails to satisfy the compact chord property. More generally, the exact equivalence between the chord and the compact chord properties is proved in [40]. Our aim in the next section is to give an equivalent characterisation of discrete straightness in the 16-neighbourhood space.
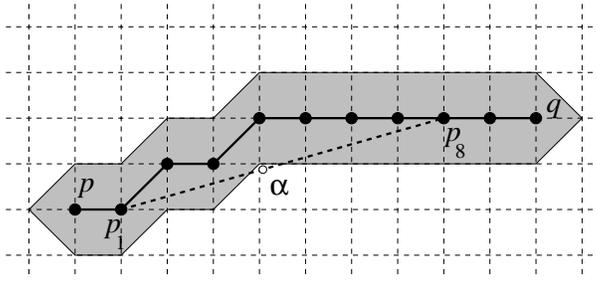
22

Figure 25: Example for the violation of the compact chord property.

5 Extensions in the 16-neighbourhood space

In order to facilitate the study of geometrical properties in the 16-neighbourhood space, we first introduce the concept of distance in this extended neighbourhood space. Two new discrete distance functions will be constructed in Section 5.1 which allow for the analytical characterisation of the 16-neighbourhood as it was the case for the City-Block and Chessboard distance in the 4- and 8-neighbourhood spaces respectively. Based on these results, a digitisation scheme is then defined that maps real straight segments onto 16-digital arcs (Section 5.2). This digitisation scheme is typically equivalent to the grid-intersect quantisation introduced previously in the 8-neighbourhood space. Finally, Section 5.3 formally characterises discrete straightness in the 16-neighbourhood space.

5.1 Definitions

In this section, we will establish an analogy between a 16-digital arc and an 8-digital arc. We introduce a transformation T_i which uniquely maps an 8-digital arc to a 16-digital arc (and vice-versa). This is motivated by the fact that the 16-digital arc does not necessarily visit the pixels on all the grid lines (vertical or horizontal) between the two end points (as deduced from Proposition 4.21). The objective would be then to define a distance in the N_{16} space, and finally, a characterisation of a 16-digital straight segment.

We define the transformation T_i on the chain code of the digital arc in question, where the subscript i indicates that the transform is chain code (*i.e.*, move) dependent. It will become apparent that this subscript indicates the octant in which the digital arc lies (*e.g.*, see Figure 26, next). We recall that the 16-chain codes are given by $\{0, 1, \cdots, 15\}$ and, using the same numbering scheme, the 8-chain codes are given by even codes $\{0, 2, 4, \cdots, 14\}$, as shown in Figure 5 (Section 3.1).

Example 5.1 T_2 transform.
We first describe the case for $i = 2$ as an example. Let P_{pq} be a 16-digital arc which is also a shortest path between p and q ($\mathrm{SP}_{16}(p, q)$). Let us assume that the slope σ of $[p, q]$ lies between 0 and $\frac{1}{2}$. This implies that P_{pq} will be composed of a-moves and c-moves. The T_2 transformation applies for the first octant codes (*i.e.*, $0 \leq \sigma \leq 1$). The analytical expression of T_2 is given by: $T_2 : (x, y) \mapsto (x \Leftrightarrow y, y)$. A chain code c represents a pair of displacements (δ_x, δ_y) in the discrete space. For this reason, we use equivalently the notation $T_i(\delta_x, \delta_y)$ and $T_i(c)$. In particular, the chain codes in N_{16} in this octant $\{0, 1, 2\}$ are mapped to the chain codes in N_8 as follows: $T_2(0) = 0$, $T_2(1) = 2$ and $T_2(2) = 4$. $\diamond$

More formally, we define the T_i transformation and its inverse T_i^{-1} for $i = 0, \cdots, 3$ representing the four octant on the right hand side of the grid shown in Figure 26 (*i.e.*, $\Leftrightarrow\infty \leq \sigma \leq +\infty$) as follows.

- $\Leftrightarrow\infty \leq \sigma \leq \Leftrightarrow 1$: $T_0 : (x, y) \mapsto (x, y + x)$ and $T_0^{-1} : (x, y) \mapsto (x, y \Leftrightarrow x)$

  $T_0(12) = 12$, $T_0(13) = 14$ and $T_0(14) = 0$

- $\Leftrightarrow 1 \leq \sigma \leq 0$: $T_1 : (x, y) \mapsto (x + y, y)$ and $T_1^{-1} : (x, y) \mapsto (x \Leftrightarrow y, y)$

  $T_1(14) = 12$, $T_1(15) = 14$ and $T_1(0) = 0$

- $0 \leq \sigma \leq 1$: $T_2 : (x, y) \mapsto (x \Leftrightarrow y, y)$ and $T_2^{-1} : (x, y) \mapsto (x + y, y)$

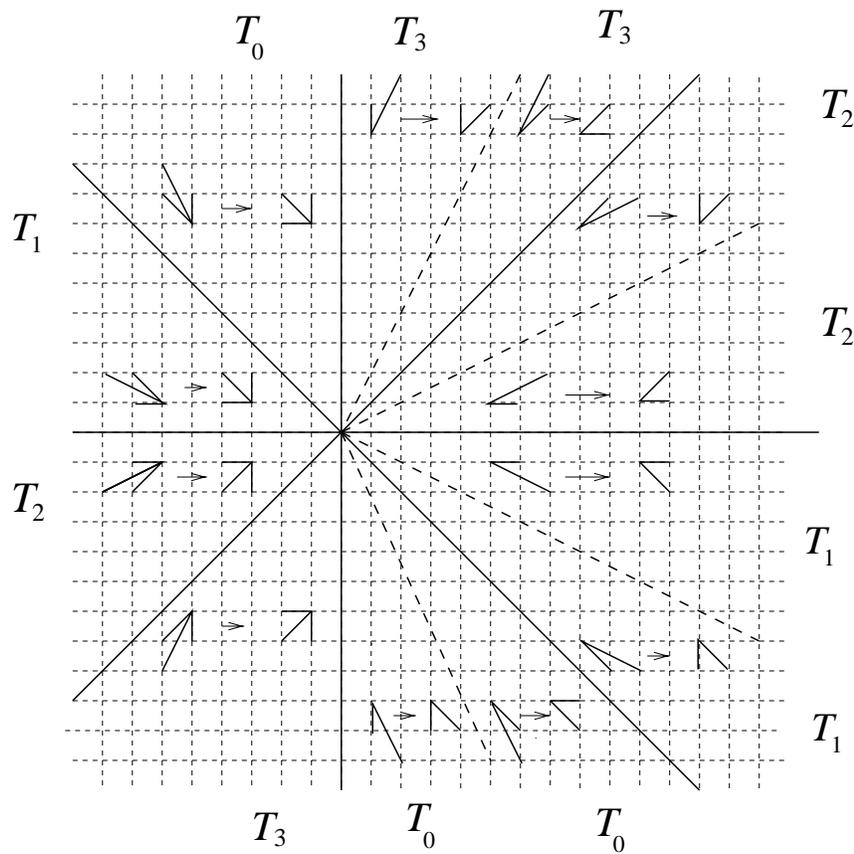 $T_2(0) = 0$, $T_2(1) = 2$ and $T_2(2) = 4$

23

Figure 26: The T_i transformation.

- $1 \leq \sigma \leq +\infty : T_3 : (x, y) \mapsto (x, y \Leftrightarrow x)$ and $T_3^{-1} : (x, y) \mapsto (x, y + x)$
  $T_3(2) = 0$, $T_3(3) = 2$ and $T_3(4) = 4$

The four other cases on the left hand side of the grid are the same by symmetry with the origin. Figure 26 depicts graphically how the 16-chain codes are transformed onto the 8-chain codes.

Thus, a 16-digital arc (*resp.* 8-digital arc) P_{pq} can be mapped onto the 8-digital arc (*resp.* 16-digital arc) $P_{p'q'}$ using the transformation: $P_{p'q'} = T_i(P_{pq})$ (*resp.* $P_{p'q'} = T_i^{-1}(P_{pq})$) where $p = p'$.

Figure 27: An example of the T_i-transform with $i = 2$.

In the case illustrated in Figure 27, P_{pq} is defined by the chain code sequence $\{0, 1, 0, 0, 1, 1\}$ and $P_{p'q'}$ is given by the chain code sequence $\{0, 2, 0, 0, 2, 2\}$.

d_4 and the d_8 distances have been established as distance functions. It was also shown in [7, 8] that N_{knight} could also be characterised by a discrete distance called d_{knight}. By contrast, the 16-neighbourhood N_{16} defined by the union of N_8 and N_{knight} cannot be simply characterised by a discrete metric (see

24

Remark 4.16). We now introduce a new distance function d_{pq} in the N_{16} space which is slope-dependent and can be seen as an extension of the City-Block distance d_4.

Definition 5.2 d_{pq} *distance.*

Given two points $p = (x_p, y_p)$ and $q = (x_q, y_q)$, we note $\delta_x(p,q) = x_q \Leftrightarrow x_p$ and $\delta_y(p,q) = y_q \Leftrightarrow y_p$. We define $d_i(p,q)$ $i = 0 \cdots 3$ as follows.

$$
\begin{aligned}
d_0(p,q) &= |\delta_x(p,q)| + |\delta_x(p,q) + \delta_y(p,q)| \\
d_1(p,q) &= |\delta_y(p,q)| + |\delta_x(p,q) + \delta_y(p,q)| \\
d_2(p,q) &= |\delta_y(p,q)| + |\delta_x(p,q) \Leftrightarrow \delta_y(p,q)| \\
d_3(p,q) &= |\delta_x(p,q)| + |\delta_x(p,q) \Leftrightarrow \delta_y(p,q)|
\end{aligned}
$$

Given two points r and s, we define $d_{pq}(r,s)$ as :

$$
d_{pq}(r,s) = d_{i^*}(r,s) \text{ with } i^* \text{ such that} : d_{i^*}(p,q) = \min_{i=0\cdots 3} d_i(p,q)
$$

Note that the value of i^* corresponds to the octant pairs defining the transformation T_i (see Figure 26).

Example 5.3 d_{pq} distance.

For example, consider the four points p, q, r and s in Figure 28. We have $\delta_x(p,q) = 10$, $\delta_y(p,q) = 3$, and hence, $d_0(p,q) = 23$, $d_1(p,q) = 16$, $d_2(p,q) = 10$ and $d_3(p,q) = 17$. Therefore, $i^* = 2$ and $d_{pq}(p,q) = d_2(p,q) = 10$.
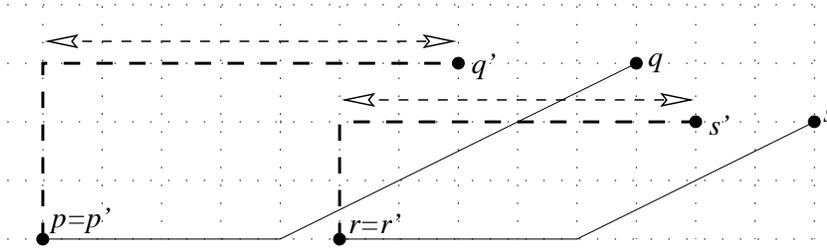

Figure 28: Distance calculations.

The definition of d_{pq} is based on the analogy with the 16-shortest path. More precisely, $d_{pq}(p,q) = l(\mathrm{SP}_{16}(p,q))$ with $a = 1$, $b = 1$ and $c = 2$. The analogy also applies to the transformed path using T_{i^*}. Indeed, $d_{pq}(p,q)$ is the length of the 4-shortest path from $p' = T_2(p)$ to $q' = T_2(q)$ with $a = b = 1$. In other words, $d_{pq}(p,q) = d_4(T_{i^*}(p), T_{i^*}(q)) = d_4(p', q')$ (dashed line).

Now, given two points r and s, for instance, we can compute $d_{pq}(r,s)$. Since $\delta_x(r,s) = 8$, $\delta_y(r,s) = 2$ then $d_{pq}(r,s) = 8$. Similarly to $d_{pq}(p,q)$, this value is the length of the 4-shortest path from $r' = T_2(r)$ to $s' = T_2(s)$ with $a = b = 1$.

In other words, $d_{pq}(r,s) = d_4(T_{i^*}(r), T_{i^*}(s)) = d_4(r', s') = 8$ (dashed line). In this example, we have chosen the slope of $[r,s]$ to be in the same octant as $[p,q]$ for simplicity. However, the distance function is general and can apply to instance when the two slopes do not belong to the same range defining i^*. $\diamondsuit$

Proposition 5.4 *The value of i^* for $d_i(p,q)$ is determined by the slope σ of the real segment $[r,s]$.*

Proof:

(i) if $\Leftrightarrow\infty < \sigma < \Leftrightarrow 1$ then
$|\delta_y(p,q)| > |\delta_x(p,q)|$ and $\delta_x(p,q).\delta_y(p,q) \leq 0$
$\Rightarrow d_0(p,q) = \min_{i=0\cdots 3} d_i(p,q)$

(ii) if $\Leftrightarrow 1 < \sigma < 0$ then
$|\delta_y(p,q)| < |\delta_x(p,q)|$ and $\delta_x(p,q).\delta_y(p,q) \leq 0$
$\Rightarrow d_1(p,q) = \min_{i=0\cdots 3} d_i(p,q)$

(iii) if $0 < \sigma < 1$ then

$$|\delta_y(p,q)| < |\delta_x(p,q)| \text{ and } \delta_x(p,q).\delta_y(p,q) \geq 0$$
$$\Rightarrow d_2(p,q) = \min_{i=0\cdots3} d_i(p,q)$$

(iv) if $1 < \sigma < +\infty$ then

$$|\delta_y(p,q)| > |\delta_x(p,q)| \text{ and } \delta_x(p,q).\delta_y(p,q) \geq 0$$
$$\Rightarrow d_3(p,q) = \min_{i=0\cdots3} d_i(p,q)$$

Similarly to the T_i transform, these values of σ (*resp.* i^*) define four octant pairs as shown in Figure 26.
$\square$

Proposition 5.5 *For a given p, q, $d_{pq}(.,.)$ is a distance function.*

Proof:

(i) $d_{pq}(r,s) = 0 \Leftrightarrow r = s$ (trivial).

(ii) $d_{pq}(r,s) = d_{pq}(s,r)$ (trivial).

(iii) $d_{pq}(r,t) \leq d_{pq}(r,s) + d_{pq}(s,t)$:

$\delta_x(r,t) = \delta_x(r,s) + \delta_x(s,t)$ and $\delta_y(r,t) = \delta_y(r,s) + \delta_y(s,t)$

then,

$|\delta_x(r,t) + \delta_y(r,t)| \leq |\delta_x(r,s) + \delta_y(r,s)| + |\delta_x(s,t) + \delta_y(s,t)|$

Likewise,

$|\delta_x(r,t) \Leftrightarrow \delta_y(r,t)| \leq |\delta_x(r,s) \Leftrightarrow \delta_y(r,s)| + |\delta_x(s,t) \Leftrightarrow \delta_y(s,t)|$

Hence, $d_{pq}(.,.)$ is a distance function.
$\square$

Proposition 5.6 $d_{pq}(p,q) = d_8(p,q)$. *Alternatively,*

$$d_{pq}(p,q) = 1 \Longleftrightarrow p \text{ and } q \text{ are 8-neighbours.}$$

Proof:

$$
\begin{aligned}
d_{pq}(p,q) &= \min\left(|\delta_x(p,q)|, |\delta_y(p,q)|\right) + ||\delta_x(p,q)| \Leftrightarrow |\delta_y(p,q)|| \\
&= \max\left(|\delta_x(p,q)|, |\delta_y(p,q)|\right) \\
&= d_8(p,q) \qquad\qquad\qquad\qquad\qquad\quad \square
\end{aligned}
$$

We can also define a new distance function D_{pq} in the N_{16} space, which can be seen as an extension of the Chessboard distance d_8. This new distance function will prove fundamental in the characterisation of the 16-neighbourhood.

Definition 5.7 D_{pq} *distance.*

Given two points $p = (x_p, y_p)$ and $q = (x_q, y_q)$, we define $D_i(p,q)$ $i = 0\cdots3$ as follows.

$$
\begin{aligned}
D_0(p,q) &= \max\left(|\delta_x(p,q)|, |\delta_x(p,q) + \delta_y(p,q)|\right) \\
D_1(p,q) &= \max\left(|\delta_y(p,q)|, |\delta_x(p,q) + \delta_y(p,q)|\right) \\
D_2(p,q) &= \max\left(|\delta_y(p,q)|, |\delta_x(p,q) \Leftrightarrow \delta_y(p,q)|\right) \\
D_3(p,q) &= \max\left(|\delta_x(p,q)|, |\delta_x(p,q) \Leftrightarrow \delta_y(p,q)|\right)
\end{aligned}
$$

Given two points r and s, we define $D_{pq}(r,s)$ as :

$$D_{pq}(r,s) = D_{i^*}(r,s) \text{ with } i^* \text{ such that : } D_{i^*}(p,q) = \min_{i=0\cdots3} D_i(p,q)$$

26

We first note that, for a given p and q, i^* which minimises the expression of d_i in the definition of d_{pq} is the same as i^* which minimises the expression of D_i in the definition of D_{pq}.

Example 5.8 D_{pq} distance.
Using the same example in Figure 28, $D_0(p, q) = 13$, $D_1(p, q) = 13$, $D_2(p, q) = 7$ and $D_3(p, q) = 10$. Hence, $i^* = 2$ and $D_{pq}(p, q) = D_2(p, q) = 7$. This value now corresponds to $d_8(p', q')$ where $p' = T_2(p)$ and $q' = T_2(q)$. In other words, $D_{pq}(p, q) = d_8(T_{i^*}(p), T_{i^*}(q)) = d_8(p', q')$ (dotted line) which establishes the analogy between D_{pq} and d_8. Likewise, $D_{pq}(r, s) = d_8(T_{i^*}(r), T_{i^*}(s)) = d_8(r', s') = 6$ (dotted line). $\diamond$

Proposition 5.9

$$D_{pq}(p, q) = 1 \iff p \text{ and } q \text{ are 16-neighbours.}$$

Proof:
Immediate by the definition of D_{pq}. $\qquad\qquad\qquad\qquad\qquad\qquad\qquad\qquad\qquad\qquad\qquad\qquad\square$

We can also easily prove that $D_{pq}(.,.)$ is a distance function, in essentially the same way as we did for $d_{pq}(.,.)$.

Figure 29 shows the different discs of radius 1 for the two new distance functions where p is the origin and q is any pixel in each quadrant of $\mathbb{Z}^2$. The disc of radius 1 is centred at pixel p (shown highlighted) and the locus of points $\alpha \in \mathbb{R}^2$ are shown shaded as given in the ccaption of Figure 29. This figure clarifies the fact that the distance metrics are defined such that they are dependent on the slope of the segment $[p, q]$. The union of discs fully describes the 16-neighbours of a pixel. Thus, D_{pq} can be used to define the N_{16} neighbourhood of a pixel explicitly.
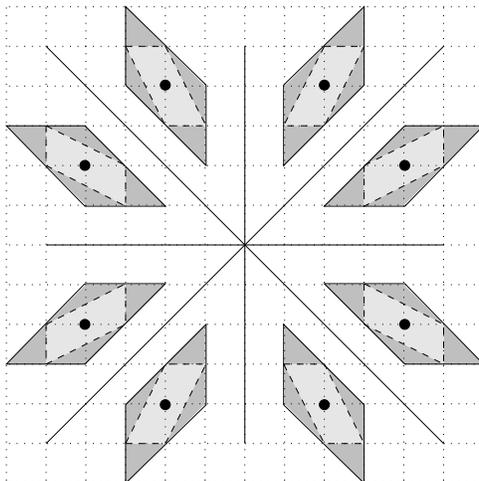

Figure 29: Bowls $d_{pq}(u, \alpha) \leq 1$ (light shaded region) and $D_{pq}(u, \alpha) \leq 1$ (dark and light shaded regions).

It will become apparent in the next sections how the newly defined distance functions will assist in reaching the goal of characterising 16-digital straight segments. We first use these distance functions d_{pq} and D_{pq} for defining a digitisation scheme that applies in the 16-neighbourhood space.

5.2   Grid-intersect quantisation GIQ_{16}

In [10], Freeman defines the grid intersection quantisation in the N_8 space (GIQ_8) using the distance d_8 as the set of pixels closest to a curve whenever it intersects a horizontal or a vertical grid line. The (8-)grid intersect quantisation of a real segment was then defined as an (8-)digital straight segment [10]. However, in the N_{16} space, because the c-move skips some grid lines, this definition is not satisfactory. We propose a new definition for the grid intersect quantisation of a real straight segment in the N_{16} space (GIQ_{16}).

Given a real segment $[\alpha, \beta]$, let p (*resp.* q) be the grid point $d_{\alpha\beta}$-closest to α (*resp.* β). Then, similarly to GIQ_8, we call $\mathrm{GIQ}_{16}(\alpha, \beta)$ the 16-digital arc which realizes the minimum area of S ($|S|$), where S is the surface between the 16-digital arc and the real segment $[\alpha, \beta]$ (see Figure 30).
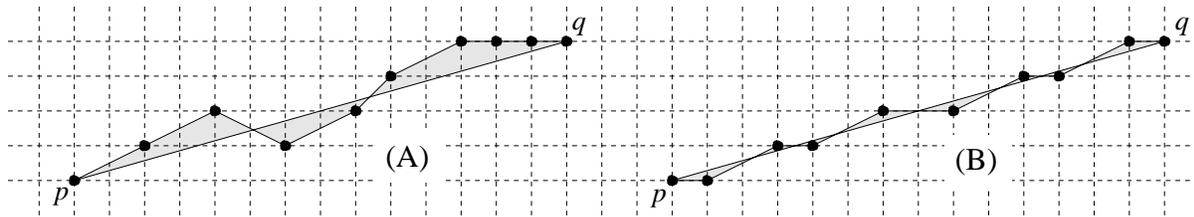
Figure 30: Surface between $[p, q]$ and the 16-digital arc. (A) Non optimal case. (B) Optimal case $(\text{GIQ}_{16}(p, q))$.

Proposition 5.10 $\text{GIQ}_{16}(\alpha, \beta)$ *is a 16-shortest path between p and q with a, b and c defined such that $d_{a,b,c}$ is a distance (see Section 4.1.1).*

Proof:
Let $\{p_0, p_1, \cdots, p_n\}$ be the set of grid points (pixels) in $\text{GIQ}_{16}(\alpha, \beta)$. Let ϕ_i be the angle between $[p, q]$ and $[p_i, p_{i+1}]$, $i = 0, \cdots n \Leftrightarrow 1$.

Thus, the minimum value of $|S|$ will be reached for the minimum value of $\sum_{i=0}^{n-1} |\phi_i|$. In turn, this also implies that each $|\phi_i|$ is also a minimum. Therefore, $\text{GIQ}_{16}(\alpha, \beta)$ will be composed of two types of moves, one with the minimum slope which is greater than the slope of $[p, q]$, and the other with the maximum slope which is smaller than the slope of $[p, q]$. In other words, the two moves are those whose slope is closest to that of $[p, q]$. Such a digital arc exists since these two moves compose $\text{SPBG}_{16}(p, q)$ as shown in Figure 14. Hence, $\text{GIQ}_{16}(\alpha, \beta)$ will be a path in $\text{SPBG}_{16}(p, q)$, and, therefore, it is a shortest path between p and q. $\qquad\square$

As a by-product of Proposition 5.10, a simpler characterisation of $\text{GIQ}_{16}(p, q)$ would be the following. $\text{GIQ}_{16}(\alpha, \beta)$ is the 16-shortest path between p and q which is closest to the real straight segment $[p, q]$. Moreover, Freeman's first criterion (Proposition 4.33(i)) can clearly be extended in the case of a 16-digital straight segment. We can deduce from Propositions 4.20 and 5.10 that $\text{GIQ}_{16}(\alpha, \beta)$ is composed of at most two directions which differ by one modulo 16. We now describe a simple algorithm for computing GIQ_{16}.

5.2.1 Implementation

Given α and β, the following algorithm will give as output $\text{GIQ}_{16}(\alpha, \beta)$:

1. Compute p and q, the $d_{\alpha\beta}$-closest pixels to α and β respectively.

2. Initialise : $P_{pq} \leftarrow \{p\}$.

3. Build a path P_{pq} by adding the next pixel p_i in $\text{SPBG}_{16}(p, q)$ closest to $[p, q]$.

4. if $p_i = q$ stop else go to step 3.

By extension of the special case of a tie in the N_8 space, we choose the lower coordinate pixel in the N_{16} space (step 3).

Proposition 5.11 *This algorithm converges and gives as output $\text{GIQ}_{16}(\alpha, \beta)$.*

Proof:
The existence of p and q is trivial. We only need to show that : For any $i > 0$, there exist two discrete points p_i and p_{i-1} adjacent in $\text{SPBG}_{16}(p, q)$ and there exists a real point δ in $[p, q]$ such that $d_{pq}(p_i, \delta) \leq \frac{1}{2}$. By induction, $p_0 = p$.

We define l and m such that $[p, q]$ crosses the line $y = x + m$ at γ and $l \Leftrightarrow \frac{1}{2} < y_\gamma < l + \frac{1}{2}$. Therefore, the next step will check for the intersection δ of $[p, q]$ with the line $y = x + m + 1$. Let σ be the slope of $[p, q]$ and let $0 < \sigma < \frac{1}{2}$. Thus, $l \Leftrightarrow \frac{1}{2} + \sigma < y_\delta < l + \frac{1}{2} + \sigma \Rightarrow l \Leftrightarrow \frac{1}{2} < y_\delta < l + 1$ If p_i is the d_{pq}-nearest point from δ then, $y_{p_i} = l$ or $y_{p_i} = l + 1$. Hence, $p_i = p_{i_1} = (x_{p_{i-1}} + 1, l)$ or $p_i = p_{i_2} = (x_{p_{i-1}} + 2, l + 1)$. Thus, $d_{pq}(p_{i_1}, p_{i_2}) = 1$ and $d_{pq}(p_{i_1}, p_{i-1}) = 1$. This means that p_{i_1} and p_{i_2} are both adjacent to p_{i-1}. Hence, the algorithm can reach either of these two points.
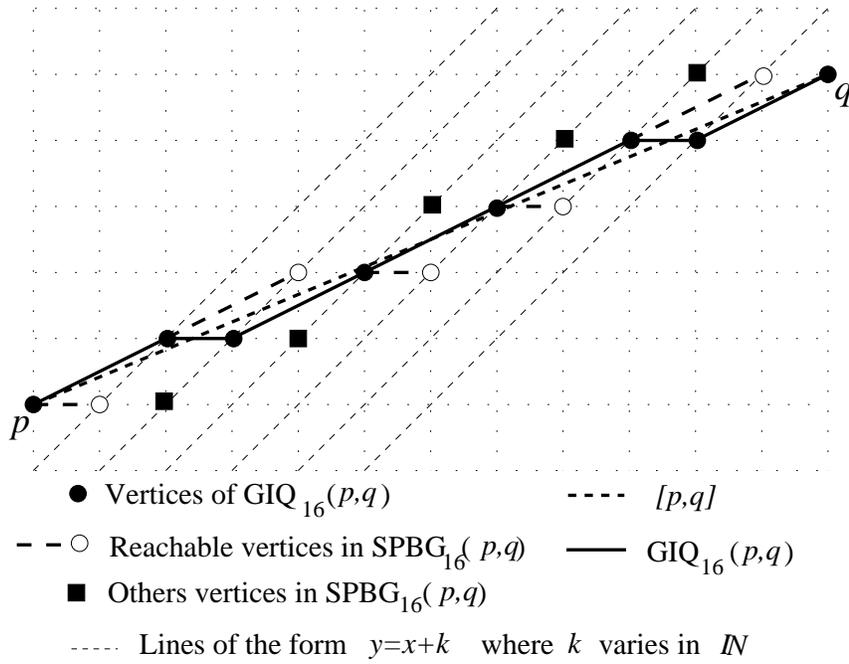
28

Figure 31: Construction of $GIQ_{16}(p,q)$.
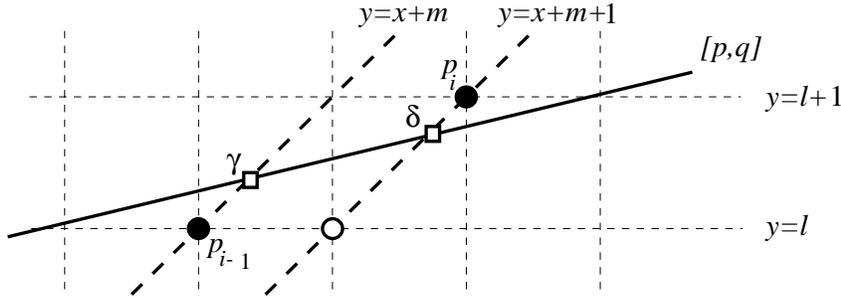

Figure 32: A step in the construction of $GIQ_{16}(p,q)$.

The end point will be the grid point closest to the crossing of $[p,q]$ with the rightmost diagonal line. By definition, it matches with q. □

5.2.2 Discrete convexity of $GIQ_{16}(p,q)$

A number of intimately linked definitions have been proposed for discrete convexity in the N_8 space on the unit square grid (see Section 4.2). We will follow the characterisation of discrete convexity given in Proposition 4.27, where a set P of grid points is said to be discrete convex if and only if $P = <P>$. The aim of this section is essentially to prove the following result.

Theorem 5.12 $GIQ_{16}(p,q)$ *is discrete convex.*

Proof:
The first remark is that $SPBG_{16}(p,q)$ contains all the points of the grid as pixels in the vicinity of $[p,q]$ (*e.g.*, see Figure 15).

Without loss of generality, we can assume that $[p,q]$ has a slope σ such that $0 < \sigma < \frac{1}{2}$. Therefore, by definition, $d_{pq}(r,s) = |(x_s \Leftrightarrow x_r) \Leftrightarrow (y_s \Leftrightarrow y_r)| + |y_s \Leftrightarrow y_r|$ and $GIQ_{16}(p,q)$ is composed of c (knight) and a (horizontal) moves (codes 0 and 1).

Let $\{p_0, p_1, \cdots, p_n\}$ be the set of discrete points in $GIQ_{16}(p,q)$. By construction of $GIQ_{16}(p,q)$, for any point p_i in $GIQ_{16}(p,q)$, there exists a real point γ in $[p,q]$ such that $d_{pq}(p_i, \gamma) \leq \frac{1}{2}$. Let $\mathcal{D} = \{\gamma \in \mathbb{R}^2$

such that $\exists \delta \in [p, q]$ such that $d_{pq}(\gamma, \delta) \leq \frac{1}{2}\}$. Then, the real convex hull of $\mathrm{GIQ}_{16}(p, q)$, $[\mathrm{GIQ}_{16}(p, q)]$ is such that $[\mathrm{GIQ}_{16}(p, q)] \subset \mathcal{D}$
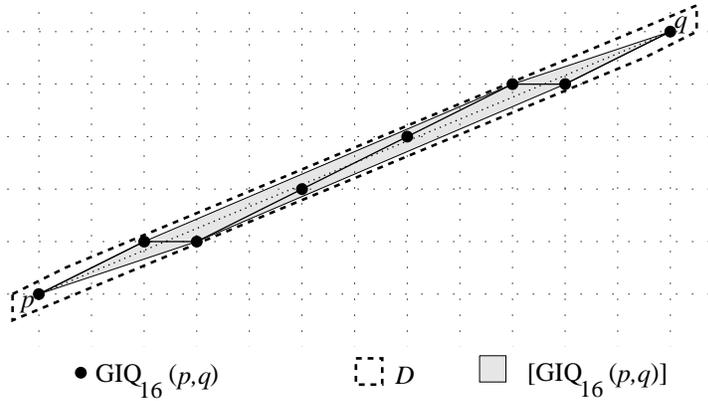

Figure 33: Verification of the discrete convexity for $\mathrm{GIQ}_{16}(p, q)$.

Let us say that a pixel p^* of $\mathrm{SPBG}_{16}(p, q)$ is such that $p^* \notin \mathrm{GIQ}_{16}(p, q)$ and $p^* \in \overset{\circ}{\mathcal{D}}$, where $\overset{\circ}{\mathcal{D}}$ is the interior of the set $\mathcal{D}$ (*i.e.*, there exists a real point γ in $[p, q]$ such that $d_{pq}(p^*, \gamma) < \frac{1}{2}$).

Since GIQ_{16} is a 16-shortest path on the grid (see Proposition 5.10), it is composed of, at most, two moves (a and c in the case of $0 < \sigma < \frac{1}{2}$). Hence, each move along GIQ_{16} crosses a line of the form $y = x + k$; $k \in \mathbb{N}$ exactly once. More precisely, on each of such lines, only one pixel p_i is such that there exists a real point $\delta \in [p, q]$ such that $d_{pq}(p_i, \delta) \leq \frac{1}{2}$ (see Figure 32). Therefore $\overset{\circ}{\mathcal{D}}$ does not contain any pixel other than those which are on $\mathrm{GIQ}_{16}(p, q)$. Consequently, the interior of the real convex hull of $\mathrm{GIQ}_{16}(p, q)$ satisfies the same property (see Figure 33). Hence, $\mathrm{GIQ}_{16}(p, q)$ is discrete convex. $\qquad\square$

5.3 Discrete straightness in the 16-neighbourhood space

In Section 4.1.2, we obtained results concerning the 16-neighbourhood coding. These result motivate the study of discrete straightness in this extended neighbourhood. In this section, our aim is to arrive at a characterisation of digital straight segments in the 16-neighbourhood space (16-digital straight segments) similar to that given by the chord properties in the 8-neighbourhood space. Based on the newly defined distances and digitisation scheme, we follow the approach taken when introducing straightness in the 8-neighbourhood space.

16-digital arcs resulting from the 16-digitisation of real straight segment are first proved to satisfy properties that belong to the class of chord properties in Section 5.3.1. The major result of this study can then be given as an analytical characterisation of 16-straightness. For the sake of completeness, Section 5.3.2 also presents the study of Upper and Lower bounds of a digital straight segment in the 16-neighbourhood space.

5.3.1 16-digital straight segments

We introduce chord properties in the extended neighbourhood space. These properties make use of the distance functions d_{pq} and D_{pq}. By analysing the construction of these distances, the new 16-chord properties will be proved to be analytical characterisations of 16-digital straight segments. Proposition 5.13 is to be compared with Propositions 4.34 and 4.38.

Proposition 5.13 *Chord properties in the 16-neighbourhood space.*

A 16-digital arc $P_{pq} = \{p_i\}_{i=0\cdots n}$ satisfies the 16-chord property if and only if, for any two discrete points p_i and p_j in P_{pq} and for any real point α on the continuous segment $[p_i, p_j]$, there exists a point $p_k \in P_{pq}$ such that $D_{pq}(\alpha, p_k) < 1$.

A 16-digital arc $P_{pq} = \{p_i\}_{i=0\cdots n}$ satisfies the 16-compact chord property if and only if, for any two discrete points p_i and p_j in P_{pq} and for any real point α on the continuous segment $[p_i, p_j]$, there exists a real point β in the broken line $\bigcup_i [p_i, p_{i+1}]$ such that $d_{pq}(\alpha, \beta) < 1$.

30

Figure 34(A) shows the geometric shapes for the 16-chord property and the 16-compact chord property. The dashed polygon (O) contains the locus of points $\alpha \in \mathbb{R}^2$ such that $D_{pq}(\alpha, P_{pq}) < 1$ and the solid polygon $(\overline{O})$ contains the locus of points $\alpha \in \mathbb{R}^2$ such that $d_{pq}(\alpha, \bigcup_i [p_i, p_{i+1}]) < 1$.

— 16-CCP (polygon $\overline{O}$)   --- 16-CP (polygon O)
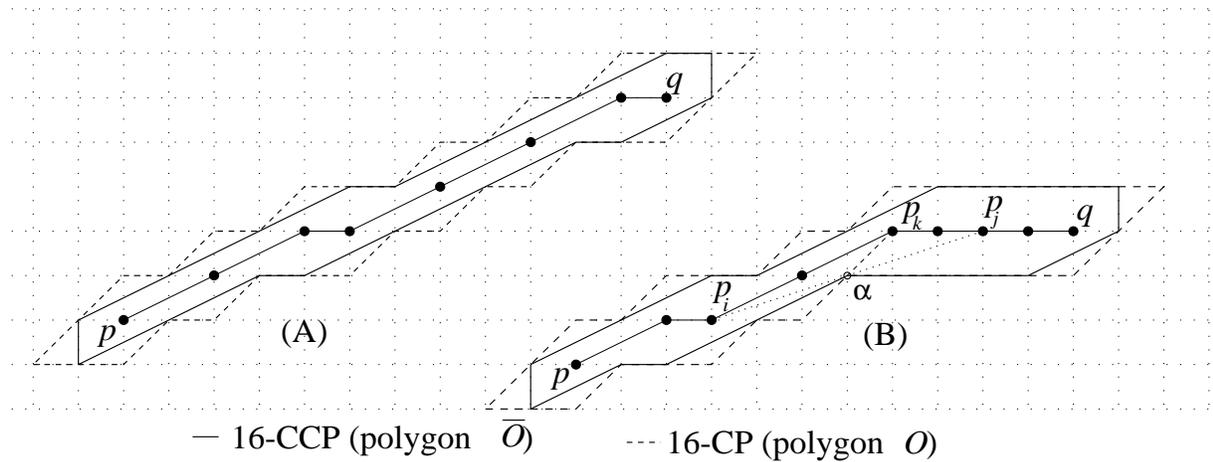
Figure 34: (A) A 16-digital arc which satisfies the 16-(compact) chord property. (B) A 16-digital arc violating the 16-(compact) chord property.

Using the concept of visibility in computational geometry, the properties can be reformulated as follows. Given two points r, s in a region $\mathcal{R}$, s is said to be strictly visible from r in $\mathcal{R}$ if the real segment $[r, s]$ is wholly contained in $\mathcal{R}$ (i.e., $[r, s]$ does not cross or touch the boundary of $\mathcal{R}$).

Proposition 5.14 *A 16-digital arc $P_{pq} = \{p_i\}_{i=0 \cdots n}$ satisfies the 16-chord property (resp. 16-compact chord property) if and only if, for any two discrete points p_i and p_j in P_{pq}, p_j is strictly visible from p_i in O (resp. in $\overline{O}$).*

Proof:
Immediate by the definition of O (resp. $\overline{O}$). □

These chord properties can now be used for characterising analytically 16-digital straight segments. We first formally define the concept of straight segment in the 16-neighbourhood space using the digitisation scheme defined earlier.

Definition 5.15 *16-digital straight segment.*
 A 16-digital arc P_{pq} is a 16-digital straight segment if there exists two real points α and β such that $\text{GIQ}_{16}(\alpha, \beta) = P_{pq}$.

The characterisation of 16-digital straight segments will be operated in two steps formulated in Lemmas 5.16 and 5.17 respectively.

Lemma 5.16 *A 16-digital straight segment satisfies the 16-compact chord property.*

Proof:
Let $P_{pq} = \{p_i\}_{i=0 \cdots n}$ be a 16-digital straight segment. By Definition 5.15, there exist two real points α and β real points such that $\text{GIQ}_{16}(\alpha, \beta) = P_{pq}$. It was shown in Section 5.2.2 that $\text{GIQ}_{16}(p, q)$ is discrete convex. In other words, if there exist two discrete points p_i and p_j in $\text{GIQ}_{16}(p, q)$ for which the 16-compact chord property is violated then, there exists a real point γ in $[p_i, p_j]$ such that for any δ in $\bigcup_i [p_i, p_{i+1}]$, $d_{pq}(\gamma, \delta) > 1$. In other words, in this case, the real convex hull of $\text{GIQ}_{16}(p, q)$, $[\text{GIQ}_{16}(p, q)]$ will contain a pixel of the $\text{SPBG}_{16}(p, q)$ which does not belong to $\text{GIQ}_{16}(p, q)$, contradicting the fact that $\text{GIQ}_{16}(p, q)$ is discrete convex.
 In Figure 34(B), the 16-compact chord property is violated. Moreover, $[\text{GIQ}_{16}(p, q)]$ contains α which is not in $\text{GIQ}_{16}(p, q)$. □

31

Lemma 5.17 *If a 16-digital arc P_{pq} satisfies the 16-compact chord property, it is a 16-digital straight segment.*

Proof:
We assume without loss of generality that the slope of $[p, q]$ is between 0 and $\frac{1}{2}$. The proof for the other cases is similar.
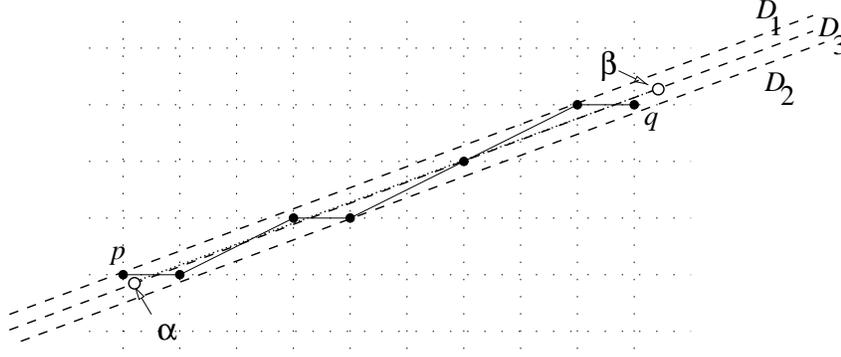

Figure 35: Characterisation of a digital straight segment.

Let $\{p_0, p_1, \cdots, p_n\}$ be the set of discrete points in P_{pq}. We define the following lines (see Figure 35):

- $\mathcal{D}_1 : y = \sigma x + \mu_1$ such that $\forall p_i \in P_{pq}$, p_i is below $\mathcal{D}_1$ $(p_i = (x_i, y_i) \Rightarrow y_i \leq \sigma x_i + \mu_1)$.

- $\mathcal{D}_2 : y = \sigma x + \mu_2$ such that $\forall p_i \in P_{pq}$, p_i is above $\mathcal{D}_2$ $(p_i = (x_i, y_i) \Rightarrow y_i \geq \sigma x_i + \mu_2)$.

$\mathcal{D}_1$ and $\mathcal{D}_2$ are defined as two parallel lines such that any point p_i in P_{pq} lies between $\mathcal{D}_1$ and $\mathcal{D}_2$. Building on this, we define a width measure for P_{pq}:

- $\mathcal{W}(\sigma, \mu_1, \mu_2) = \min(d_{pq}(\delta, \varepsilon) \mid \delta \in \mathcal{D}_1 \; ; \; \varepsilon \in \mathcal{D}_2)$.

- $\mathcal{W}^* = \mathcal{W}(\sigma^*, \mu_1^*, \mu_2^*) = \min_{\sigma, \mu_1, \mu_2}(\mathcal{W}(\sigma, \mu_1, \mu_2))$. ($\mathcal{W}^*$ is the minimal d_{pq}-width of P_{pq}).

Now, to prove Lemma 5.17, we only need to prove that there exists a real straight segment $[\alpha, \beta]$ where $d_{pq}(\alpha, p) < \frac{1}{2}$ and $d_{pq}(\beta, q) < \frac{1}{2}$ such that $\text{GIQ}_{16}(\alpha, \beta) = P_{pq}$. In this context, it is then sufficient to prove that, if P_{pq} satisfies the 16-compact chord property then $\mathcal{W}^* < 1$.

By definition, one of the two lines $\mathcal{D}_1$ and $\mathcal{D}_2$ ($\mathcal{D}_1$, say) contains at least two points p_i and p_j from P_{pq} and the other line ($\mathcal{D}_2$), contains at least one point p_k from P_{pq}. Otherwise, $\mathcal{W}^*$ would not be minimal. For obtaining a minimal width ($\mathcal{W}^*$), one of $\mathcal{D}_1$ or $\mathcal{D}_2$ should be a part of the real convex hull of P_{pq}, as shown schematically in Figure 36(A).

Now, let η be a point on $\mathcal{D}_1$ such that $d_{pq}(p_k, \eta)$ is minimum (*i.e.*, $d_{pq}(p_k, \eta) = \mathcal{W}^*$). For the triangle $\Delta p_i p_j p_k$ to have a minimal width $\mathcal{W}^*$, η should be a point on $[p_i, p_j]$ (see Figure 36(B)). Hence, p_k lies between p_i and p_j on the 16-digital arc P_{pq} (*i.e.*, $p_k \in P_{p_i p_j} \subseteq P_{pq}$).
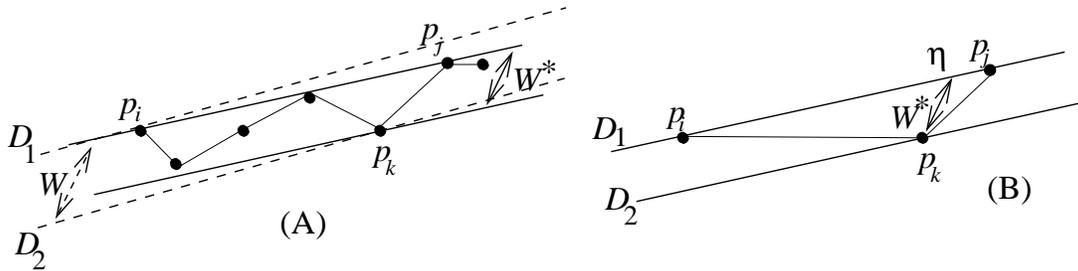

Figure 36: Geometrical evidence.

Now, if P_{pq} satisfies the 16-compact chord property then clearly $P_{p_i p_j} \subseteq P_{pq}$ satisfies the 16-compact chord property. Moreover, since $p_k \in P_{p_i p_j}$, there exists $\gamma \in [p_i, p_j]$ (*i.e.*, on $\mathcal{D}_1$) such that $d_{pq}(p_k, \gamma) < 1$.

Hence, there exist $\gamma \in \mathcal{D}_1$ and $\delta \in \mathcal{D}_2$ such that $d_{pq}(\gamma, \delta) < 1$. Since $\mathcal{D}_1$ and $\mathcal{D}_2$ are two parallel lines, we obtain $\mathcal{W}^* < 1$.

Let $\mathcal{D}_3$ be the line $y = \sigma x + \frac{\mu_1 + \mu_2}{2}$. $\mathcal{D}_3$ is both parallel and d_{pq}-equidistant to $\mathcal{D}_1$ and $\mathcal{D}_2$. Hence, for any $p_i \in P_{pq}$, there exists $\gamma \in \mathcal{D}_3$ such that $d_{pq}(\delta, p_i) < \frac{1}{2}$.

Let α and β be two real points on $\mathcal{D}_3$ such that $d_{pq}(p, \alpha) < \frac{1}{2}$ and $d_{pq}(q, \beta) < \frac{1}{2}$, respectively. Then, $GIQ_{16}(\alpha, \beta) = P_{pq}$. Therefore, for each digital arc which satisfies the 16-compact chord property we can define a real segment (not unique) such that its grid-intersect quantisation is the digital arc in question. In other words, a digital arc which satisfies the 16-compact chord property is a 16-digital straight segment. $\square$

Combining the above results, we conclude this study of 16-straightness with the following main result.

Theorem 5.18 *A 16-digital arc is a digital straight segment if and only if it satisfies the 16-compact chord property.*

Proof:
The necessary condition is given by Lemma 5.16 and the sufficient condition is given by Lemma 5.17. $\square$

5.3.2 Upper and Lower bounds of $[p, q]$

In [26], Pham defined the (8-)Upper and Lower bound digital arcs for a given real segment and proved that they define two (8-)digital straight segments. Their construction is based on shifting chain-codes of the Grid-Intersect quantisation of the real segment in question. These bounds allow for locating all possible digital straight segments joining two discrete points. We can easily extend these definitions to the 16-neighbourhood. In the algorithm defined in Section 5.2, at each step, at most two pixels can be reached in $SPBG_{16}(p, q)$ (see Figures 15 and 32). We will say that one of these pixels defines the 16-Upper bound if it is above $[p, q]$ while the other pixel defines the 16-Lower bound (see Figure 37).
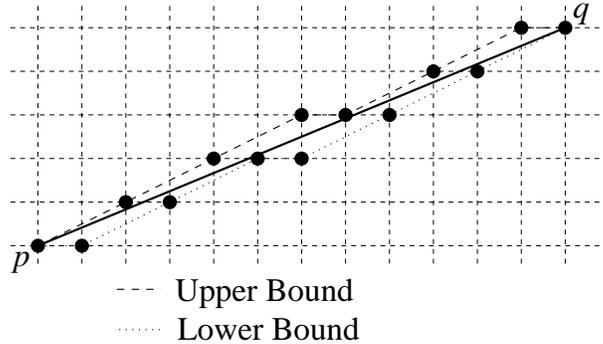

--- Upper Bound
...... Lower Bound

Figure 37: Upper and Lower bounds.

Proposition 5.19 *The 16-Upper and 16-Lower bounds define two 16-digital straight segments.*

Proof:
The 16-Upper and 16-Lower bounds are two 16-shortest paths since they are defined in the $SPBG_{16}(p, q)$. Let $U_{pq} = \{u_0, \cdots, u_n\}$ and $L_{pq} = \{l_0, \cdots, l_m\}$ be the 16-Upper bound and 16-Lower bound respectively. By definition, $\forall i \in \{0, \cdots, n\}$ there exists $r \in P_{pq}$ such that $d_{pq}(r, u_i) \leq 1$

We can therefore define the same surface $\mathcal{D}$ as in Section 5.2.2 where $[p, q]$ is included in the border of $\mathcal{D}$. It is then immediate to see that U_{pq} satisfies the 16-compact chord property.

More precisely, if we define a real segment $[\alpha, \beta]$ as the medial line of $\mathcal{D}$, then clearly, $GIQ_{16}(\alpha, \beta) = U_{pq}$. Hence, U_{pq} is a digital straight segment. The proof for the case of L_{pq} is obtained by symmetry. $\square$

Further properties defined in the 8-neighbourhood space find their equivalent in the 16-neighbourhood space. The intimate link with combinatorial structures defined in this study and the duality created by T_i transforms readily suggest these extensions.

In the next section, we present an example of such a mapping applied to the problem of vectorisation of chain-code sequences.

6 Application to vectorisation

In this section, we suggest two algorithms for the polygonal decomposition of a 16-digital path. For illustrating the developments presented in this study, we propose two algorithms for checking for the straightness of digital arcs. Applications of such algorithms include vectorisation of binary line images (*e.g.*, engineering drawings).

Two approaches are taken. Section 6.1 first proposes a direct application of chord properties. This results in a greedy (*i.e.*, suboptimal) decomposition of the 16-digital arc in question.

Optimal polygonal approximation algorithms exist in the 8-neighbourhood space. With the same token as in Section 5.3.2, we propose in Section 6.2 to exploit the duality created by T_i transforms for enabling such procedures to operate equivalently on 16-digital arcs.

6.1 A greedy algorithm

This algorithm tests the straightness of P_{pq} in a greedy fashion. Each time the straightness is violated, another 16-digital straight segment is stacked. The algorithm returns Λ, the list of break points for all the 16-digital straight segments in P_{pq} and N_Λ the number of 16-digital straight segments. In this case, N_Λ is not necessarily minimum.

Given a 16-digital arc $P_{pq} = \{p_0, p_1, \cdots, p_n\}$:

1. $i, j, N_\Lambda \leftarrow 0$; $\Lambda \leftarrow \{p_0\}$

2. $j \leftarrow j + 1$

3. If $j > n$ then $\Lambda \leftarrow \Lambda \cup \{p_n\}$; $N_\Lambda \leftarrow N_\Lambda + 1$; Stop.

4. Compute the slope of $[p_i, p_j]$ to determine an expression for $d_{p_i p_j}(.,.)$.

5. Check the visibility of the pixel p_j against the pixels $\{p_i, p_{i+1}, \cdots, p_{j-1}\}$
   in the polygon $\{\alpha \in \mathbb{R}^2 \text{ such that } \exists \beta \in \bigcup_i [p_i p_{i+1}] \text{ such that } d_{p_i p_j}(\alpha, \beta) < 1\}$.

   - If p_j is visible from all these pixels then goto step 2.
   - else:
     (a) $\Lambda \leftarrow \Lambda \cup \{p_{j-1}\}$
     (b) $N_\Lambda \leftarrow N_\Lambda + 1$.
     (c) $i \leftarrow j$ goto step 2.

6.2 Checking discrete straightness using the duality generated by T_i

The validity of the next proposition is based of the continuity and reversibility properties of transformations T_i.

Proposition 6.1 *Given a 16-digital arc P_{pq}, let σ be the slope of $[p, q]$. Using the suitable index $i^* \in \{0, 1, 2, 3\}$ (i.e. depending on σ, see definition of T_i in Section 5.1), the following holds:*

- *P_{pq} satisfies the 16-chord property if and only if the 8-digital arc $T_{i^*}(P_{pq})$ satisfies the 8-chord property.*

- *P_{pq} satisfies the 16-compact chord property if and only if the 8-digital arc $T_{i^*}(P_{pq})$ satisfies the 8-compact chord property.*

Example 6.2 Duality.
Proposition 6.1 can be illustrated using the example shown in Figure 38 where $i^* = 2$. $\diamond$

From Proposition 6.1, we can readily define an algorithm which tests for 16-digital straightness by combining the use of transformations T_i and existing procedures that check for discrete straightness in the N_8 space (*e.g.*, [9, 21, 37, 38, 41]).
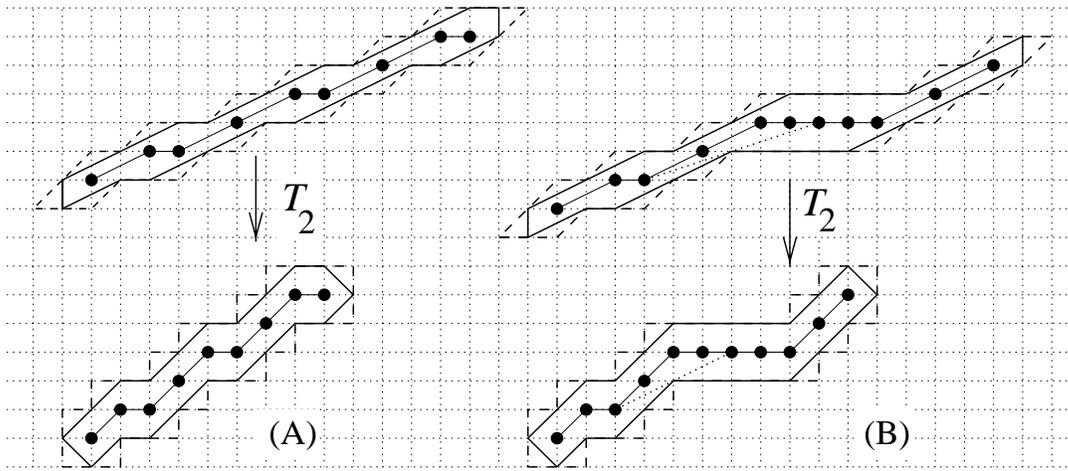
Figure 38: (A) The chord properties hold. (B) The chord properties are violated.

7 Conclusion

In this paper, we aimed to introduce techniques for analysing data in discrete spaces. In particular, we concentrated in binary digital image processing where the only information available is the (0-1) value of a pixel at a discrete location.

The mapping of continuous data into a discrete space and the construction of an underlying topological structure for the discrete space were detailed in the first sections. Then, based on connectivity relationships formally established between discrete points, we detailed the study of typical geometrical properties of connected sets. We then mapped these results into an extended discrete space. This was essentially based on the rigorous characterisation of a mapping between 8- and 16-neighbourhood spaces. This study resulted into a formal characterisation of discrete straightness in the 16-neighbourhood space. We also showed that such an approach allowed to map and extend further results into the 16-neighbourhood space.

The study of digital data in discrete spaces allows for a better understanding of problems encountered when operating digitisation. It is important to follow such a discrete approach from the basis of an analysis to be able to control and overcome approximations associated with discrete data processing.

Although applied solely to binary images, this context can be extended to other types of images with essentially no fundamental modification. For example, geodesic distances, leading to DTOCS [44] in gray scale images are an instance of an extension of discrete distances presented in this paper.

References

[1] G. Borgefors. Distance transformations in arbitrary dimensions. *Computer Vision, Graphics and Image Processing*, 27:321–345, 1984.

[2] G. Borgefors. Distance transformations in digital images. *Computer Vision, Graphics and Image Processing*, 34:344–371, 1986.

[3] J.-M. Chassery. Discrete convexity: definitions, parametrization and compatibility with continuous convexity. *Computer Vision, Graphics and Image Processing*, 21:326–344, 1983.

[4] J.-M. Chassery and M. I. Chenin. Topologies on discrete spaces. In Simon and Haralick, editors, *Digital Image Processing*, pages 59–66. Reidel Publ., 1980.

[5] J.-M. Chassery and A. Montanvert. *Géométrie Discrète en Analyse d'Images*. Editions Hermès, Paris, 1991. (in French).

[6] N. Christofides, H. O. Badra and Y. M. Sharaiha. Data structures for topological and geometric operations on networks. *Annals of Operations Research: OR/IS Interface*, 71:259–289, 1997.

[7] P. P. Das and B. N. Chatterji. Knight's distances in digital geometry. *Pattern Recognition Letters*, 7:215–226, 1988.

[8] P. P. Das and J. Mukherjee. Metricity of super knight's distance in digital geometry. *Pattern Recognition Letters*, 11:601–604, 1990.

[9] L. Dorst and A. W. M. Smeulders. Discrete representation of straight lines. *IEEE Transactions on Pattern Analysis and Machine Intelligence*, PAMI-6(4):450–463, 1984.

[10] H. Freeman. Boundary encoding and processing. In B. S. Lipkin and A. Rosenfeld, editors, *Picture Processing and Psychopictorics*, pages 241–266. New York Academic, 1970.

[11] H. Freeman. Computer processing of line-drawing images. *Computing Surveys*, 6(1):57–97, 1974.

[12] M. Gondran and M. Minoux. *Graphs and algorithms*. Wiley-Interscience Series in Discrete Mathematics. John Wiley and Sons, 1984.

[13] F. Harary, R. A. Melter and I. Tomescu. Digital metrics: a graph-theoretical approach. *Pattern Recognition Letters*, 2:159–163, 1984.

[14] C. J. Hilditch and D. Rutovitz. Chromosome recognition. *Annals of the New York Academy of Sciences*, 157:339–364, 1969.

[15] S. H. Y. Hung. On the straightness of digital arcs. *IEEE Transactions on Pattern Analysis and Machine Intelligence*, PAMI-7(2):203–215, 1985.

[16] C. E. Kim. On the cellular convexity of complexes. *IEEE Transactions on Pattern Analysis and Machine Intelligence*, PAMI-3:617–625, 1981.

[17] C. E. Kim. Digital convexity, straightness and convex polygons. *IEEE Transactions on Pattern Analysis and Machine Intelligence*, PAMI-4:618–626, 1982.

[18] C. E. Kim and A. Rosenfeld. Digital straight lines and convexity of digital regions. *IEEE Transactions on Pattern Analysis and Machine Intelligence*, PAMI-4(2):149–153, 1982.

[19] C. E. Kim and J. Sklansky. Digital and cellular convexity. *Pattern Recognition*, 15:359–367, 1982.

[20] T. Y. Kong and A. Rosenfeld. Digital topology: introduction and survey. *Computer Vision, Graphics and Image Processing*, 48:357–393, 1989.

[21] M. Lindenbaum and J. Koplowitz. A new parametrisation of digital straight lines. *IEEE Transactions on Pattern Analysis and Machine Intelligence*, PAMI-13:847–852, 1991.

[22] S. Marchand-Maillet and Y. M. Sharaiha. Euclidean ordering via chamfer distance calculations. Submitted to *Computer Vision and Image Understanding*, 1997.

[23] U. Montanari. A method for obtaining skeletons using a quasi-Euclidean distance. *Journal of the ACM*, 15(4):600–624, 1968.

[24] U. Montanari. A note on minimal length polygonal approximation to a digitized contour. *Communications of the ACM*, 13:41–47, 1970.

[25] O. J. Morris, M. de Jersey Lee and A. G. Constantinides. Graph theory for image analysis: An approach based on the shortest spanning tree. *IEE Proceedings-F Communications Radar and Signal Processing*, 133(2):146–152, 1986.

[26] S. Pham. Digital straight segments. *Computer Vision, Graphics and Image Processing*, 36:10–30, 1986.

[27] C. Ronse. Definitions of convexity and convex hulls in digital images. *Bull. Soc. Math. Belge Série B*, 37(2):71–85, 1985.

[28] C. Ronse. An isomorphism for digital images. *Journal of Combinatorial Theory, Series A*, 39:132–159, 1985.

[29] C. Ronse. A simple proof of Rosenfeld's characterisation of digital straight segments. *Pattern Recognition Letters*, 3(5):323–326, 1985.

[30] C. Ronse. A topological characterization of thinning. *Theoretical Computer Science*, 43:31–41, 1985.

[31] C. Ronse. A strong chord property for 4-connected convex digital sets. *Computer Vision, Graphics and Image Processing*, 35:259–269, 1986.

[32] C. Ronse. A bibliography on digital and computational convexity (1961-1988). *IEEE Transactions on Pattern Analysis and Machine Intelligence*, PAMI-11(2):181–189, 1989.

[33] A. Rosenfeld. Digital straight line segments. *IEEE Transactions on Computers*, C-23(12):1264–1269, 1974.

[34] A. Rosenfeld. Digital topology. *American Mathematical Monthly*, 86:621–629, 1979.

[35] A. Rosenfeld and R. A. Melter. Digital geometry. *The Mathematical Intelligencer*, 11(3):69–72, 1989.

[36] A. Rosenfeld and J. L. Pfaltz. Distances functions on digital pictures. *Pattern Recognition*, 1:33–61, 1968.

[37] Y. M. Sharaiha. *A graph theoretic approach for the raster-to-vector problem in digital image processing*. PhD thesis, Imperial College, London, 1991.

[38] Y. M. Sharaiha and N. Christofides. An optimal algorithm for straight segment approximation of digital arcs. *CVGIP: Graphical Models and Image Processing*, 55(5):397–407, 1993.

[39] Y. M. Sharaiha and N. Christofides. A graph theoretic approach to distance transformations. *Pattern Recognition Letters*, 15(10):1035–1041, 1994.

[40] Y. M. Sharaiha and P. Garat. A compact chord property for digital arcs. *Pattern Recognition*, 26(5):799–803, 1993.

[41] A. W. M. Smeulders and L. Dorst. Decomposition of discrete curves into piecewise straight segments in linear time. In A. Rosenfeld R.A. Melter and P. Batthacharaya, editors, *Vision Geometry, Contemporary Mathematics*, pages 169–195. American Mathematical Society, Providence, RI, 1991.

[42] S. Suzuki, N. Ueda and J. Sklansky. Graph-based thinning for binary images. *International Journal of Pattern Recognition and Artificial Intelligence*, 7(5):1009–1030, 1993.

[43] E. Thiel and A. Montanvert. Chamfer masks: discrete distance functions, geometrical properties and optimization. In *Eleventh International Conference on Pattern Recognition*, pages 244–247, The Hague, The Netherlands, August 30–September 3 1992.

[44] P. J. Toivanen. New geodesics distance transform for grayscale images. *Pattern Recognition Letters*, 17:437–450, 1996.

[45] K. Voss. *Discrete images, objects and functions in $\mathbb{Z}^n$*. Algorithms and Combinatorics, 11. Springer Verlag, Berlin, 1993.